International Journal of Bifurcation and Chaos, Vol. 6, No. 1 (1996) 119–148

MULTI-PARAMETER CRITICALITY IN CHUA'S CIRCUIT AT PERIOD-DOUBLING TRANSITION TO CHAOS

A. P. KUZNETSOV, S. P. KUZNETSOV and I. R. SATAEV
Institute of Radio Engineering and Electronics, Russian Academy of Sciences, Zelenaya 38, Saratov, 410019, Russia

L. O. CHUA
Department of Electrical Engineering and Computer Sciences, University of California, Berkeley, CA, 94720, USA

Received April 1, 1995; Revised September 25, 1995

Investigation of non-Feigenbaum types of period-doubling universality is undertaken for a single Chua's circuit and for two systems with a unidirectional coupling. Some codimension-2 critical situations are found numerically that were known earlier for bimodal 1D maps. However, the simplest of them (tricritical) does not survive in a strict sense when the exact dynamical equations are used instead of the 1D map approximation. In coupled systems double Feigenbaum's point and bicritical behavior are found and studied. Scaling properties that are the same as in two logistic maps with a unidirectional coupling are illustrated.

1. Introduction

Many nonlinear systems exhibit transition to chaos according to Feigenbaum's scenario via the period-doubling bifurcation cascade. The simplest representative of this class is the logistic map

$$x_{n+1} = 1 - \lambda x_n^2 . \qquad (1)$$

In this example the period-doubling bifurcation sequence $\lambda = 0.75, 1.25, 1.36809\ldots$ converges to the limit value $\lambda_c = 1.4011552\ldots$ which is called a *critical point.* This is usually referred to as a threshold of chaos. Feigenbaum has discovered that the remarkable properties of universality and scaling are valid at the critical point and in its neighborhood [Feigenbaum, 1978, 1979]. In state space (the x axis) and in the parameter space (the λ axis) self-similar patterns can be detected. They reproduce themselves under rescaling with the universal Feigenbaum's constants $\alpha = -2.5029\ldots$ and $\delta = 4.6692\ldots$, respectively (Fig. 1). Feigenbaum has also developed the appropriate theoretical technique, *the renormalization group (RG) approach,* which gives an explanation of the universality and scaling phenomena.

For a multi-parameter analysis of transition to chaos, we must study the parameter space of dimension N_p, where N_p is the number of control parameters. The presence of Feigenbaum's scenario means that we observe a series of codimension-1 surfaces in the parameter space. The period-doubling bifurcations occur at these surfaces, and they converge to a limit called Feigenbaum critical set; which is also a codimension-1 surface. (Depending on N_p we may have a Feigenbaum's surface, curve, or point.) However, the multi-parameter analysis is much more complicated. For example, in the two-parameter case the boundary of chaos may contain not only the Feigenbaum's critical curves but also special

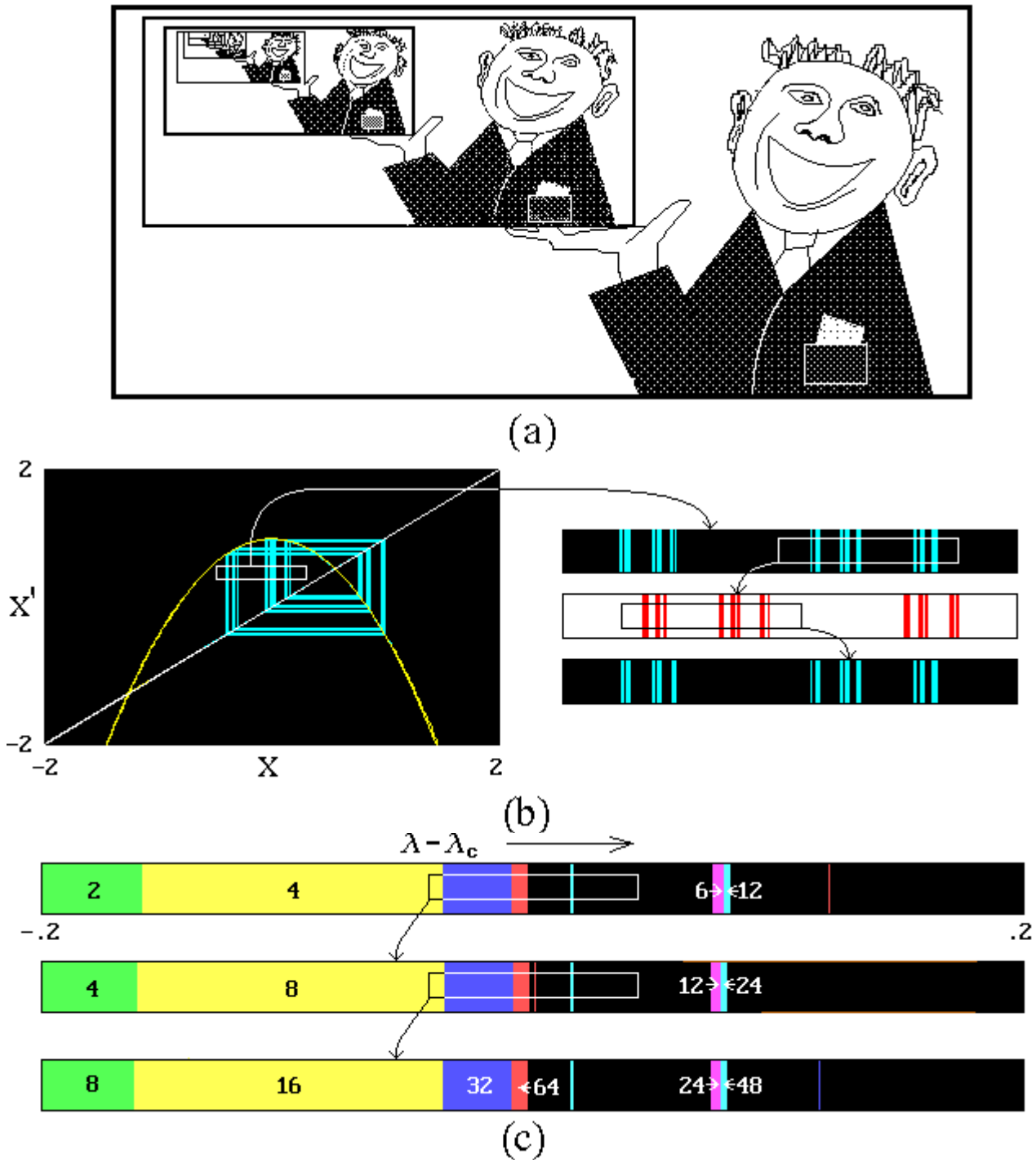

Fig. 1. General idea of scaling (a) and its manifestation in the dynamics of the logistic map. Attractor pictured in the iteration diagram (b) exhibits a Cantor-like structure that reproduces itself at each second step of magnification by the universal factor $|a_F| = 2.5029\ldots$. In (c) the pattern of the one-dimensional parameter space (λ axis) is shown. Colors represent different periods (marked by numbers) for regular stable motions. The black region corresponds to chaos and unresolved high-period cycles. The period-doubling accumulation limit — Feigenbaum's critical point — is located exactly at the center. The topographic pattern is reproduced under magnification by the factor $\delta = 4.6692$ and by doubling all characteristic timescales.

critical points of codimension-2: In a neighborhood of such a point the scaling properties are different from Feigenbaum's. For three-parameter systems we may find Feigenbaum critical surfaces, critical curves (whose occurrence is revealed by two-parameter analysis), and new types of behavior at critical points of codimension-3. As we increase the number of control parameters, new types of critical

behavior emerge that must be taken into account as generic phenomena.

We suppose that the dynamical behavior at each of these critical sets of different codimensions allows an RG analysis and gives rise to a class of quantitative universality and scaling. If this is the case, the parameter space topography near the critical point (curve, surface) will be universal and will depend only on the type of criticality. This parameter space pattern may appear in many systems of different nature and may be considered as a multi-parameter generalization of the concept of "road to chaos" or "scenario".

This research program on the "theory of multi-parameter criticality" goes back to A. Poincaré. He supposed that in mathematical disciplines we have to consider phenomena in an order of increasing codimension: At first, only the generic case, then the cases which appear typically in one-parameter families, then the typical cases when two parameters are involved, and so on. In bifurcation theory and catastrophe theory, powerful mathematical foundations have been developed using such an approach. However, in studying multi-parameter criticality we have to use (at least for now) numerical calculations, in addition to some essential ideas from the RG analysis.

We already know a number of non-Feigenbaum examples of period-doubling criticality: In 1D maps (bimodal and with cubic inflection point [MacKay & van Zeijts, 1988; Kuznetsov *et al.*, 1993b; Kuznetsov *et al.*, 1994a, 1994b]), in area-preserving 2D maps [Helleman, 1980; Eckmann *et al.*, 1982; Lichtenberg & Lieberman, 1982], in non-invertible 2D maps (among them in a system of two 1D maps with a unidirectional coupling) [Bezruchko *et al.*, 1986; Kuznetsov *et al.*, 1991, 1993a; Kuznetsov & Sataev, 1992]. Until now, most examples on this subject are concerned with model systems, such as artificially constructed maps. On the other hand, Feigenbaum's criticality has been observed in a large number of real physical systems and differential equations. So, the fundamental question for the theory of multi-parameter criticality is: Do the non-Feigenbaum critical situations occur in real physical systems as well as in contrived abstract maps? We discuss this question here. The basic example will be Chua's circuit, which is a remarkable proving ground for a variety of ideas and approaches in nonlinear dynamics [Chua *et al.*, 1986; Madan, 1993]. In Sec. 2 we compare three methods which have been used to investigate various aspects of Chua's circuit: Differential equations, exact 2D Poincaré map, and approximate Chua's 1D map. We discuss here Feigenbaum's critical behavior of Chua's circuit, which represents one of the simplest case of criticality and a paradigm for further considerations. In Sec. 3 we find in Chua's system some codimension-2 criticality types known earlier only for 1D bimodal maps. In Sec. 4 we show that two Chua's systems may be used to obtain the criticality types discovered in two 1D maps with a unidirectional coupling.

2. Chua's Circuit: Dynamics in Terms of Differential Equations and Maps. Feigenbaum's Criticality in Chua's System

Chua's circuit is a simple electronic system which contains a nonlinear resistor (Chua's diode) with a piecewise-linear characteristic [Chua *et al.*, 1986; Madan, 1993]. The dynamics is governed by the equations

$$\begin{aligned} \frac{dx}{dt} &= \alpha(y - h(x))\,, \\ \frac{dy}{dt} &= x - y + z\,, \\ \frac{dz}{dt} &= -\beta y\,. \end{aligned} \tag{2}$$

where x, y, z are dynamical variables, α and β are normalized dimensionless parameters, and $h(x)$ is a function chosen in accordance to Chua *et al.* [1986] in the following form:

$$\begin{aligned} h(x) &= (1+b)x + a - b\,,\ x \geqslant 1\,, \\ &= (1+a)x\,,\ -1 \leqslant x \leqslant 1\,, \\ &= (1+b)x - a + b\,,\ x \leqslant 1\,, \end{aligned} \tag{3}$$

where traditionally the parameters a and b are fixed: $a = -8/7$ and $b = -5/7$.

Depending on α and β the system (2) exhibits a variety of periodic and chaotic regimes. The dynamical behavior may be best summarized by plotting a "geographical map" in the parameter plane. In Fig. 2 such a diagram is presented from a computer solution of Eqs. (2), in addition to some typical portraits of attractors calculated at some parameter points. (We use a modified parameter plane (α', β) with $\alpha' = \alpha = -0.68\beta$ simply for better visualization.) Different colors show domains of distinct stable periodic motions. The black sea region is occupied mostly by chaos, except for rather

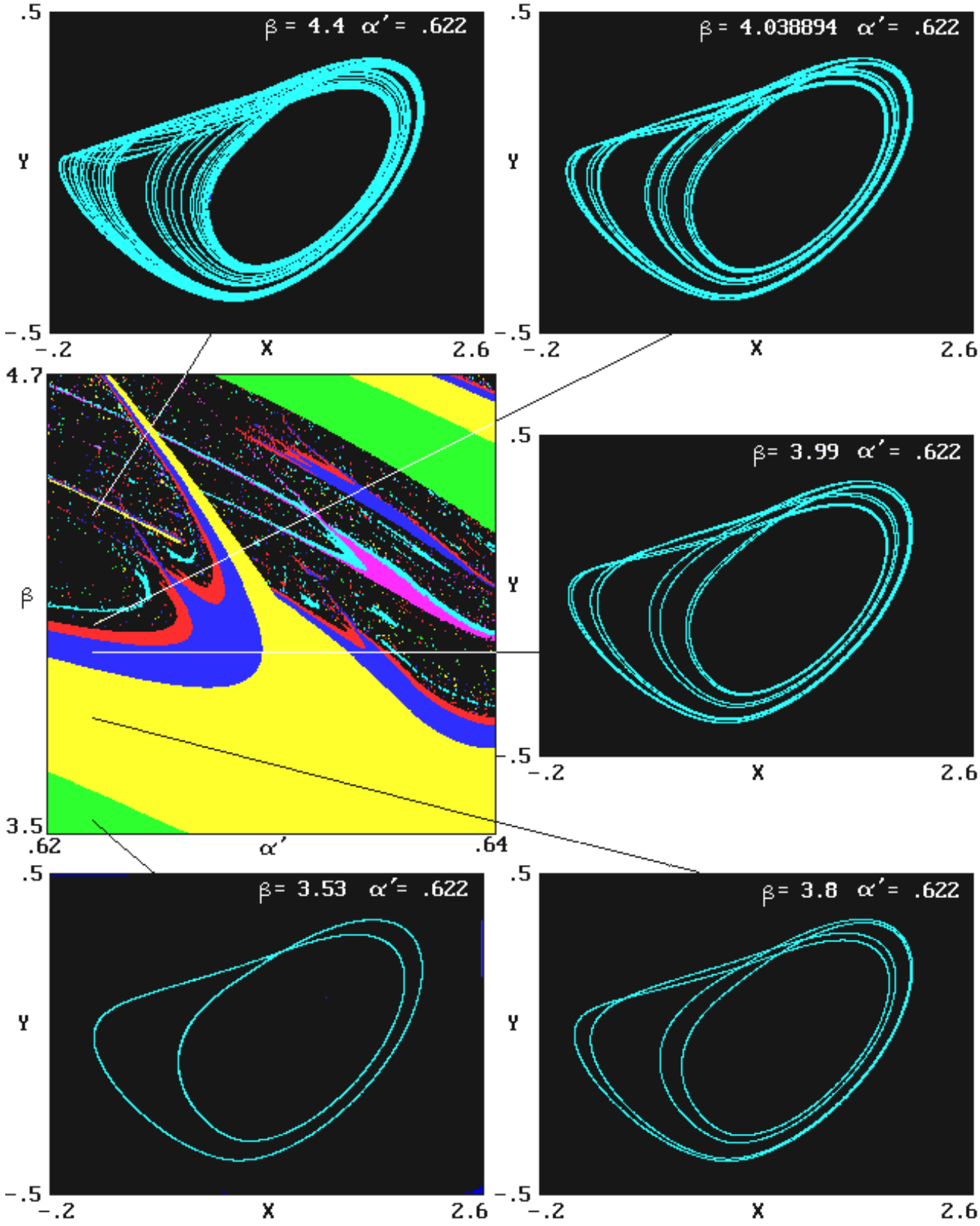

Fig. 2. Topography of the parameter plane for Chua's system (2) and portraits of attractors in the projection onto the (x, y) plane. Colors in the parameter plane represent distinct stable periodic regimes: green – period $2T$, yellow – $4T$, violet – $8T$, red – $16T$, pink – $6T$ and light blue – $12T$, where T is the basic period which depends slightly on the parameters α' and β. The black area is occupied mostly by chaos. Top portraits of the attractors correspond to chaos (left) and the threshold of chaos (right). The other attractors correspond to periodic motions.

small domains (not shown) corresponding to cycles of longer periods. If we vary only one parameter of the circuit, we will move apparently along a certain path (a one-parameter curve) in the parameter plane. The typical scenario of transition to chaos in such a case is a classic period-doubling cascade. The attractors shown in Fig. 2 correspond to only a few sample parameter points of the evolution from periodicity to chaos along the vertical line $\alpha' = 0.622$.

Now let us consider Poincaré's idea of using maps instead of differential equations. In the 3D state space of Chua's circuit (x, y, z) we select a surface (plane) in such a way that it would intersect transversally the flow of phase trajectories (Fig. 3). Taking any point in the cross section, we can trace the orbit emanating from this point until it again visits the surface at some other point. The associated 2D mapping of the surface into itself is called a Poincaré map. Now we may set aside the initial system (differential equations) and use the Poincaré map. It reproduces the dynamics exactly (we did not use any approximations) but details of the dynamics between subsequent visits of the Poincaré surface are omitted. In general, the Poincaré map can only be constructed numerically, but for Chua's circuit it was found analytically by Chua *et al.* [1986] (see Appendix 1).

In this paper we shall use the terminology *Chua's system* to mean either the differential equations (2), or its *exact* 2D Poincaré map.

In Fig. 3 we show several plots of attractors for Chua's system (2) and the location of the Poincaré section according to Chua *et al.* [1986]. The intersections of the trajectories with the Poincaré surface are shown on the right-hand side.

It appears that for the chosen parameter values the dissipation in Chua's system is strong. This means that the contraction of an infinitesimal phase volume is quite large over the time period between subsequent visits of the Poincaré surface. This circumstance makes it possible to go from the exact to an approximate description of the dynamics in terms of a 1D map.

Due to the strong dissipation, the points of the attractors on the Poincaré section of Fig. 3 are localized along rather narrow and stretched strips. Let us define the coordinates on the Poincaré surface in such a way that the X-axis is directed along the strip, and the Y axis transversal to it. Then the exact 2D Poincaré map

$$X' = G(X, Y), \quad Y' = F(X, Y), \tag{4}$$

may be approximated by Chua's 1D map

$$X' = G(X), \tag{5}$$

where $G(X) = G(X, O)$, whose analytical representation is rather cumbersome (see Chua *et al.* [1986]; Genot [1993], and Appendix 1).

It is clear that the form of the $G(X)$ function depends on the parameters α and β from the original Eq. (2). In Fig. 4 we reproduce again the topography of the parameter plane, but now for Chua's 1D map. One can see an excellent correspondence with Fig. 2: It seems impossible to find visible differences. Several iteration diagrams are presented for this 1D map from selected sample points on the parameter plane. Observe that the trajectories in Fig. 2 and the diagrams in Fig. 4 are qualitatively identical.

We see from Fig. 4 that the dynamics of the 1D map evolves in a neighborhood of the quadratic extremum. Hence, it is not surprising that the classic period-doubling scenario occurs. In Appendix 2, we reproduce briefly the RG analysis for 1D maps (it will be necessary also for the next section). Feigenbaum's universality appears due to the following fact: Under appropriate variable changes, at the critical point we obtain a convergence of the 2^k-fold iterated maps to the limit function $g(x)$. This function is the fixed point of the RG transformation (or doubling transformation). This means that $g(x)$ satisfies the following Feigenbaum's functional equation

$$g(x) = ag\left(g\left(\frac{x}{a}\right)\right), \tag{6}$$

where $a = -2.5029\ldots$. The dynamics of small perturbations of this fixed point under the doubling transformation is governed by a unique eigenvalue, the universal Feigenbaum's constant $\delta = 4.6692\ldots$.

It is important to note that for the exact description of dynamics in terms of differential equations, or its associated 2D Poincaré map, the quantitative universality of period-doubling cascade remains valid. The mathematical proof of Feigenbaum's conjecture was given by Collet, Eckmann & Koch [1981].

In Table 1, we give the period-doubling bifurcation values of β at the line $\alpha' = 0.622$, both for Chua's 1D map and for exact equations. Also the precise coordinates of the critical points are presented there. Figure 5 demonstrates the universal convergence law of the bifurcation sequence: In logarithmic scale, the points relating to Chua's system

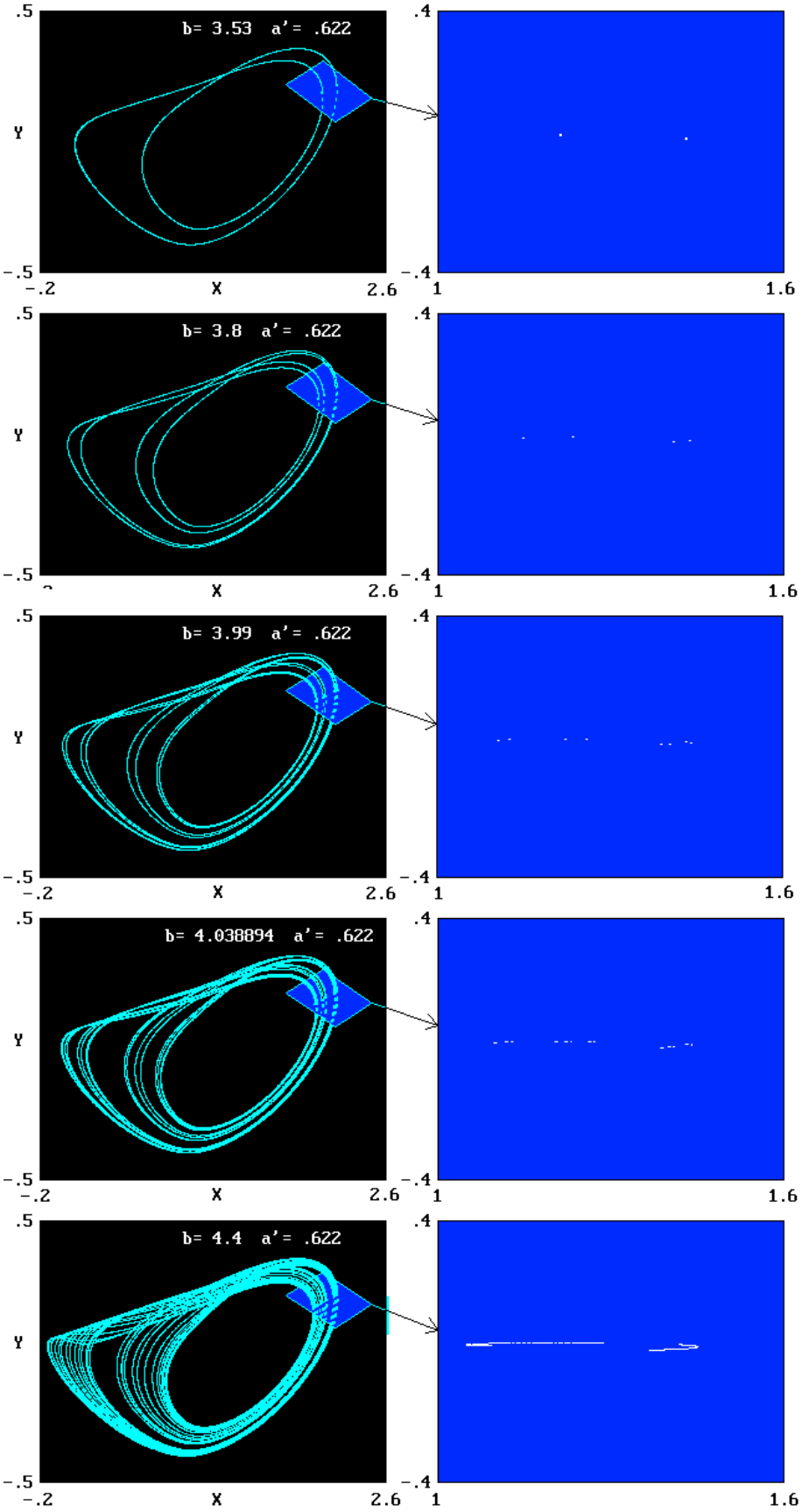

Fig. 3. Portraits of attractors for Chua's system (2) (left column), shown with the position of Poincaré section according to Chua *et al.* [1986]. The right column shows figures appearing in the cross section. Note that the points on the Poincaré section are located along narrow strips due to strong dissipation.

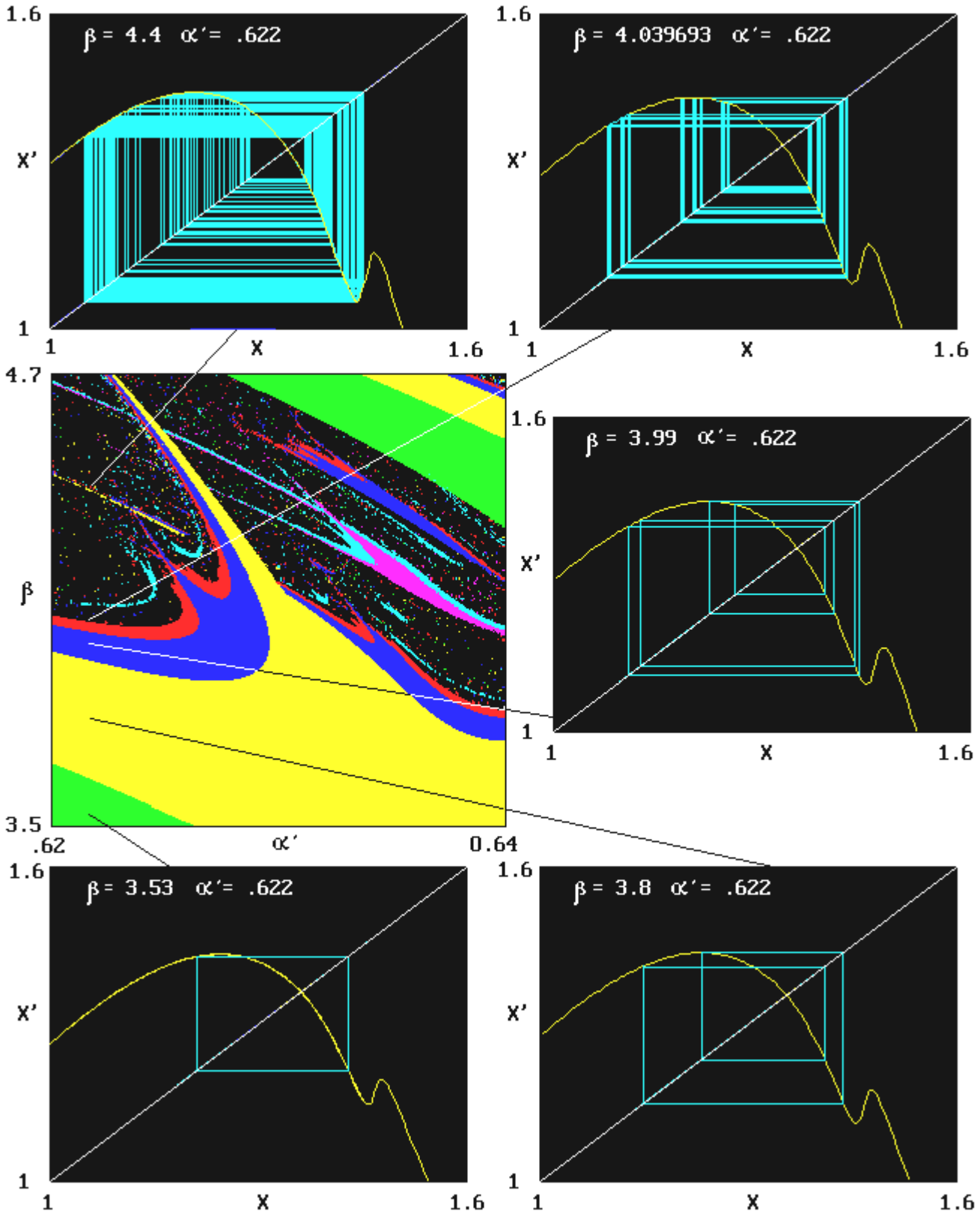

Fig. 4. Topography of the parameter plane for Chua's 1D map and iteration diagrams at some particular points. Colors in the parameter plane represent distinct stable periodic regimes: green – period 2, yellow – 4, violet – 8, red – 16, pink – 6 and light blue – 12. Top iteration diagrams correspond to chaos (left) and threshold of chaos (right). The other diagrams correspond to periodic motions.

Table 1. Parameter β values for period-doubling bifurcations for Chua's system and 1D Chua's map with $\alpha' = 0.622$.

N	1D Chua's Map	Chua's System
2	3.666848032	3.665888963
4	3.953550920	3.952745109
8	4.020713819	4.019915529
16	4.035606822	4.034808200
32	4.038816816	4.038018012
64	4.039505438	4.038706590
128	4.039652968	4.038854110
256	4.039684567	4.038885706
β_c	4.039693179	4.038894317

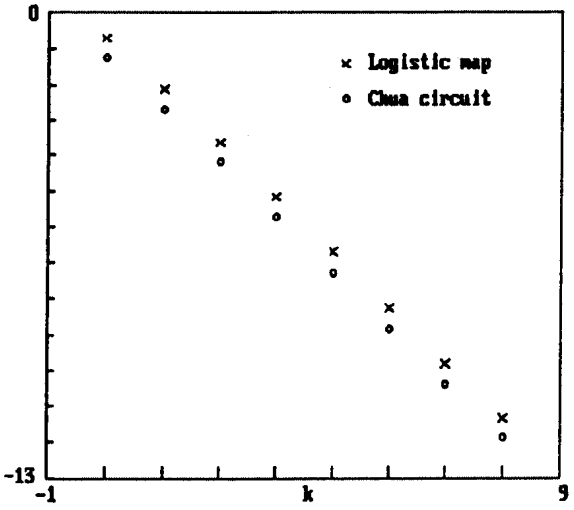

Fig. 5. Illustration of Feigenbaum's convergence law for logistic map (1) and Chua's system (2): Doubling bifurcation number versus logarithm of differences of subsequent bifurcation values.

and to the logistic map fall in parallel straight lines (the slope is expressed through Feigenbaum's δ).

Figure 6 shows the topography of the parameter plane for the exact Chua's equations (2). Two small areas are shown with magnification to illustrate Feigenbaum's scaling. One can see that the same one-dimensional pattern appears when we increase the magnification by a factor equal to δ. The only difference consists of a doubling of time scales for all observed regimes.

In Fig. 7(a), an iteration diagram is presented for Chua's 1D map calculated at its critical point. A small inset of the picture is shown on the right with a magnification equal to Feigenbaum's universal factor 2.5029.... Observe that the configuration of "strips" forming the attractor is self-similar and repeats itself at each second step of magnification. Actually, this is a Cantor-like set that was studied by many authors. Its Hausdorff dimension was found to be $D = 0.538040...$ (See, for example, Halsey *et al.* [1986].) In Fig. 7(b) a phase portrait is shown for Eqs. (2), calculated at the critical point (the parameters α and β are slightly different from the case of Chua's 1D map). We see again the same Cantor-like structure reproducing itself under magnification. Apparently, the Hausdorff dimension of this attractor is equal to $D + 1$. (An integer 1 is added to D due to the presence of a longitudinal direction, along the phase trajectories. For the corresponding set of points observed in the Poincaré section the dimension would be equal to D.)

We restrict ourselves to this brief discussion of Feigenbaum's critical behavior. This is the simplest and a well-studied type of period-doubling criticality. For further references in this paper, we designate it by a symbol F. In particular, we will use this subscript to denote the Feigenbaum's universal numbers.

3. Codimension-2 Critical Points Intrinsic to 1D Bimodal Map in Chua's System

Let us return to Fig. 2 where the parameter plane topography was shown for Chua's system. Observe that the boundary of chaos in the parameter plane is a rather complicated object (see also [Komuro *et al.*, 1991; Carcasses *et al.*, 1991; Kuznetsov *et al.*, 1993b]. There exist many cusps, and each cusp gives rise to two emanating fold lines that correspond to hard transitions (jumps). Along folds narrow strips of periodicity penetrate far into the black sea that is occupied by chaos.

What peculiarities of dynamics are responsible for such a nature of chaos boundary? As we have mentioned, the same picture (at least, visually) is demonstrated also by Chua's 1D map. For 1D maps such a picture appears typically if there are two extrema in the region of the 1D state space where the dynamics evolves. Such maps are called *bimodal*. Looking at the plots of Chua's 1D map (Fig. 4) one can conclude that this is indeed the case.

Now let us review the principal ideas for analyzing period-doubling in bimodal 1D maps. It was developed by Fraser & Kapral [1984], MacKay and van Zeijts [1988], and particularly for Chua's map by Kuznetsov *et al.* [1993b]. The so-called

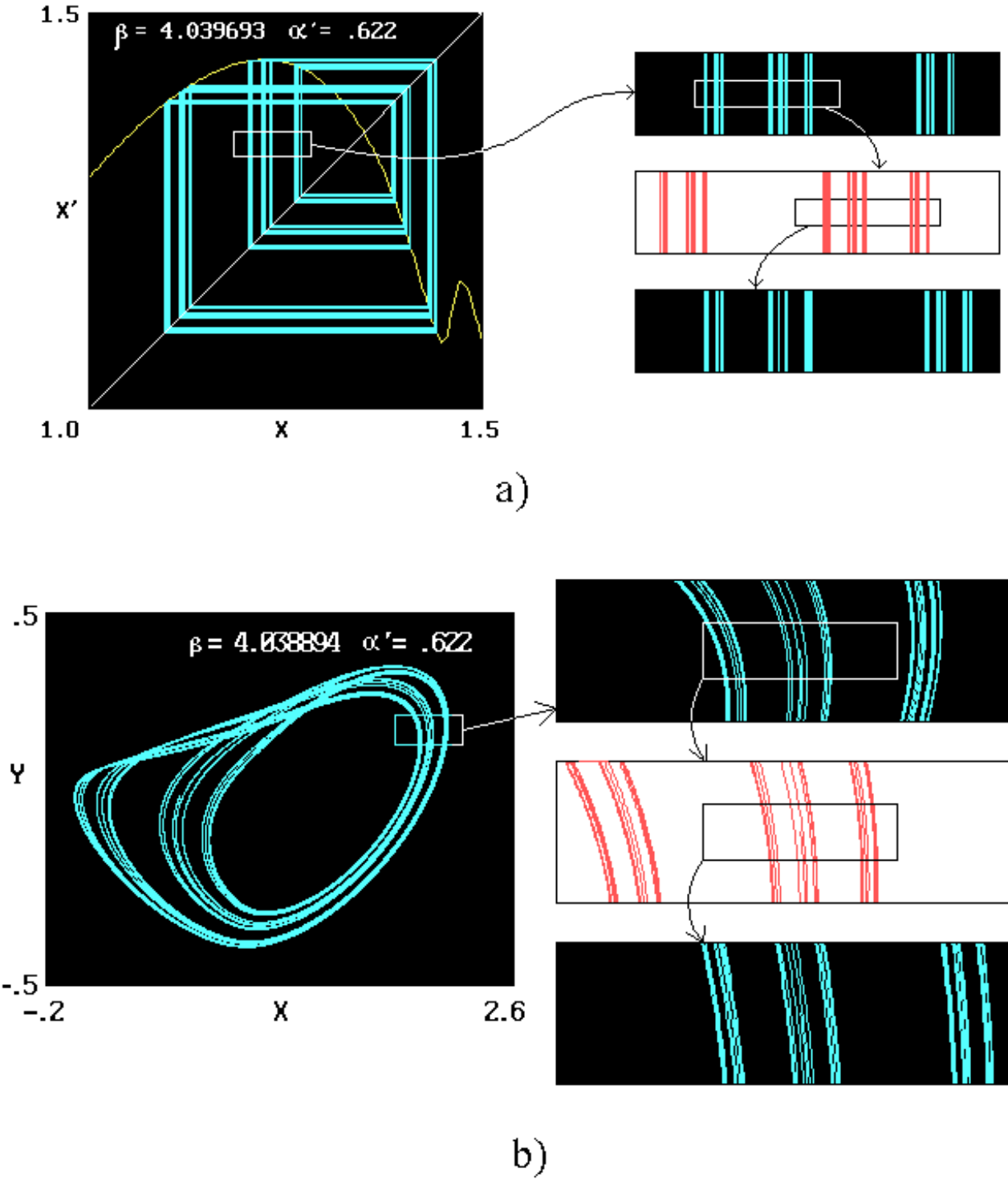

Fig. 6. Iteration diagram for Chua's 1D map (a) and portrait of attractor for Chua's system at their Feĭgenbaum's critical points. A Cantor-like self-similar structure is seen under increasing resolution. The magnification factor for parts shown separately is $|a_F| = 2.5029$. The pictures reproduce itself at each second step.

double superstable cycles play an important role here. These cycles occur at particular points in the parameter plane at which the periodic orbit contains both extremum points of the 1D map. If the maximum is mapped to the minimum after p iterations, and the minimum is mapped to the maximum after q iterations, then we call the orbit a (p, q)-*type double superstable cycle*. Its period is evidently $p+q$. The point in the parameter plane where such a cycle exists may be obtained at the intersection of two curves, $u(p)$ and $d(q)$. The curve $u(p)$ is defined by the condition that starting from the maximum the orbit arrives at the minimum after p iterations. Conversely, for the curve $d(q)$, the orbit

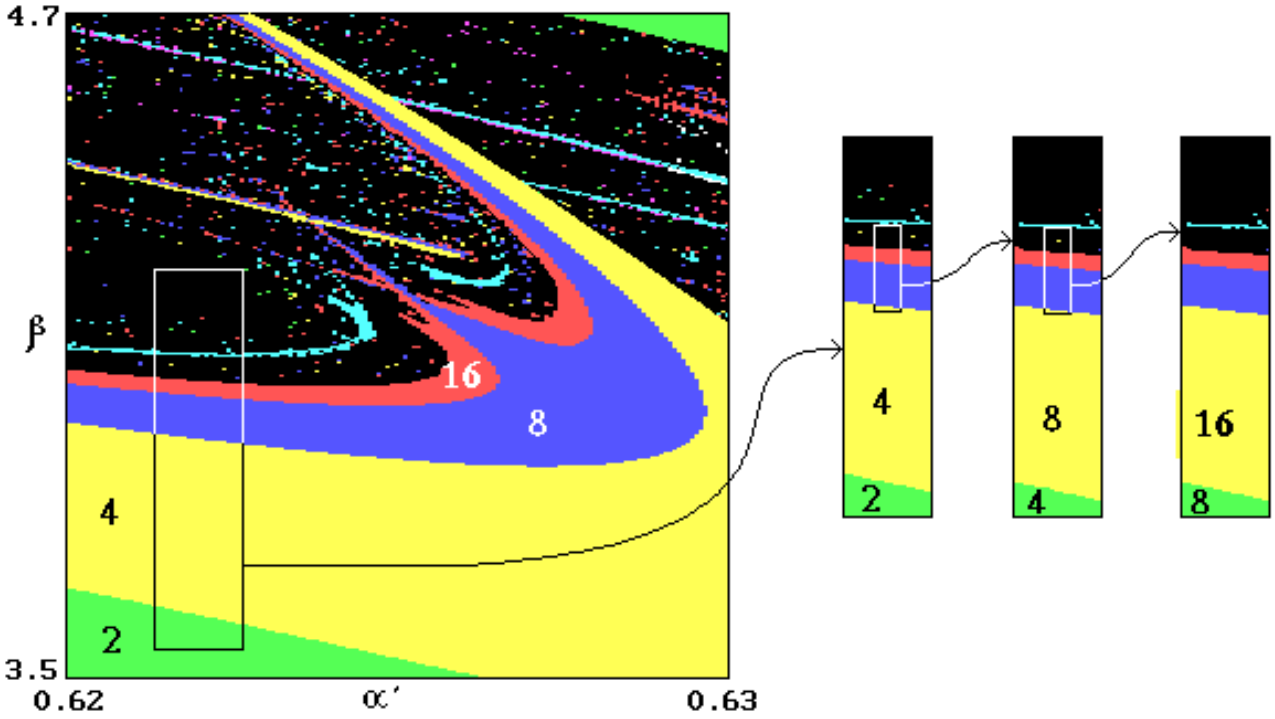

Fig. 7. One-parameter scaling in a neighborhood of Feigenbaum's critical curve in the parameter plane of Chua's system (2). The magnification factor for parts shown separately is $\delta_F = 4.6692$.

traverses from the minimum to the maximum after q steps. Moving in the parameter plane from a point of double superstable cycle along the curve $u(p)$ we observe along this curve a period-doubling bifurcation, and after that we find a new point where again a double superstable cycle appears. Its type will be $(p, p + 2q)$. In addition, moving along the curve $d(q)$ we should find a new double superstable cycle of type $(2p + q, q)$. Each of these two points again gives rise to two new branches u and d, and so on. Hence, in the parameter plane we obtain a *binary tree* consisting of u and d curves. The branching points of the tree correspond to double superstable cycles. In Fig. 8 we show the configuration of this tree, calculated numerically from Chua's 1D map.

To deal with different itineraries on the binary tree we introduce a coding system with two symbols U and D. An itinerary with any arbitrary code $UDUDDU\ldots$ corresponds to a unique route along the binary tree. The double superstable cycles that appear on this route are of the types that may be found from the code according to the rule:

$$p_{k+1}=p_k\,,\ q_k+1=2q_k+p_k\,,\ \text{if the subsequent symbol is } U\,,$$
$$p_{k+1}=2p_k+q_k\,,\ q_{k+1}=q_k\,,\ \text{if the subsequent symbol is } D\,. \qquad (7)$$

For an infinite UD-string the double superstable cycles obtained from this rule correspond to a sequence of points in the parameter plane that converges to a certain codimension-2 critical point. The law of period-doubling accumulation along the path to such a point differs from that of Feigenbaum's route to chaos.

Universality and scaling properties for codimension-2 critical points may be found from the RG analysis developed by MacKay & van Zeijts [1988]. A simplified version based on a straightforward extension of Feigenbaum's approach was considered in our previous work [Kuznetsov *et al.*, 1993b]. It is summarized briefly in Appendix 2.

The simplest kind of codimension-2 critical behavior takes place for UD-codes having a tail with a unique repeating symbol, U or D. Such codes correspond to the so-called *tricritical points* which were designated by a symbol T [Chang *et al.*, 1981; Fraser & Kapral, 1983; Kuznetsov, 1994]. It may be concluded from the binary tree construction that the tricritical behavior occurs when some iteration of the original map accepts a quartic extremum rather than a quadratic one. Tricritical points actually appear to be the end points of Feigenbaum's critical curves. Tricriticality is associated with certain (different from Feigenbaum's) fixed point of the RG equation (6) with a scaling constant $a = -1.6903\ldots$. In the parameter plane of the 1D map two-parameter scaling takes place near a tricritical point. This means that in appropriate

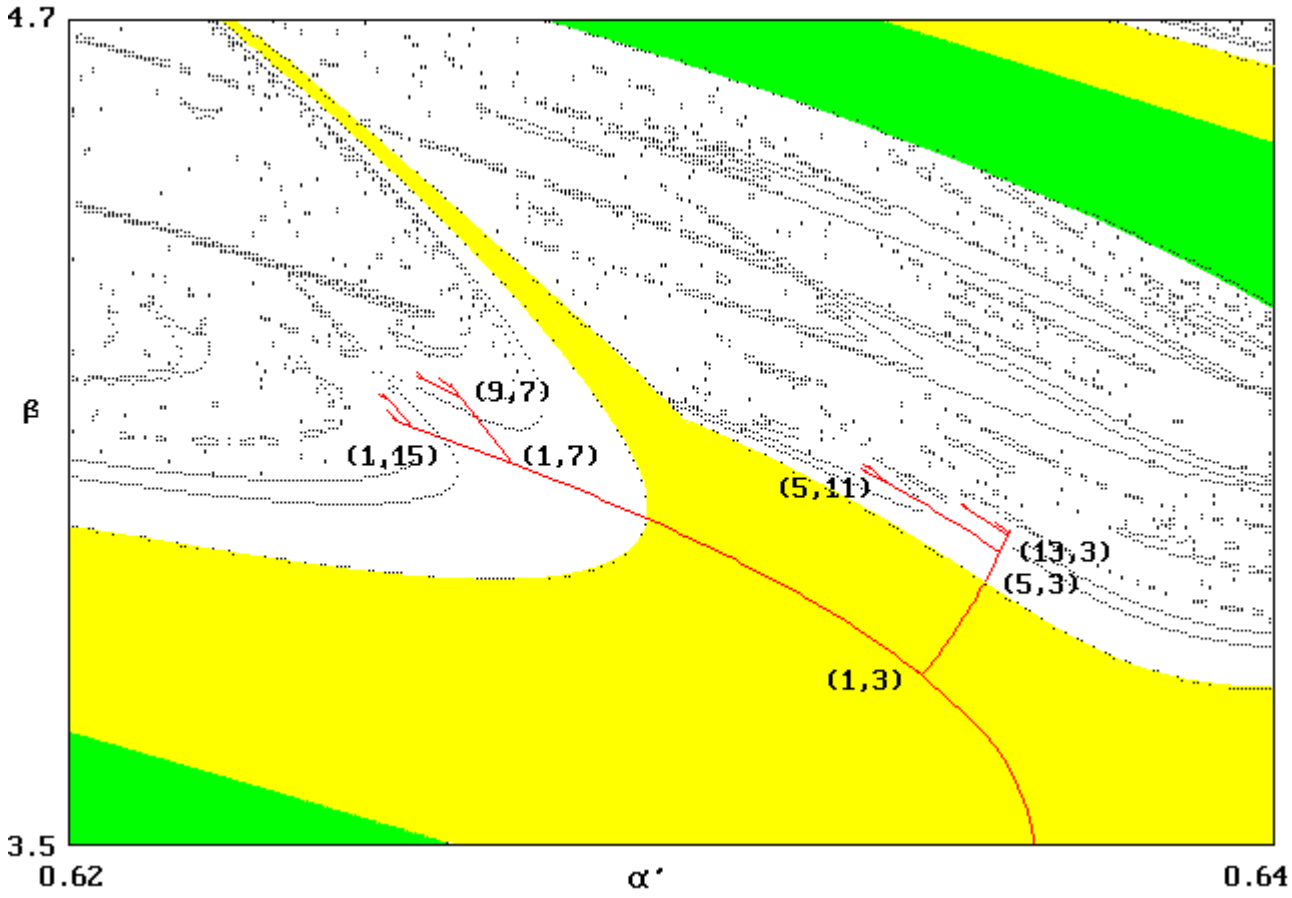

Fig. 8. Location of the binary tree in the parameter plane of Chua's 1D map superimposed upon the background of the topography reproduced from Fig. 4.

coordinates the local topography reproduces itself under a scale changed by certain factors, $\delta_1 = 7.284\ldots$ and $\delta_2 = 2.857\ldots$. Under such magnification we should see the same topographic pattern but with a doubling time scale in all regimes.

If a code tail has a period $K = 2, 3, 4\ldots$ then the behavior at the critical point is associated with a saddle solution of the RG equation (A2.2) that is a period-K cycle. In this case the parameter plane also has a self-similar topography near the critical point. Scaling factors depend on the *UD*-code, and the similarity of the dynamics is observed for time scales multiplied by a factor of 2^k.

Finally, random *UD*-sequences correspond to *non-periodic* saddle solutions of the *RG* equation. They give rise to critical points that do not exhibit a self-similar local topography in the parameter plane. Only scaling in a statistical sense may be observed. We will not discuss such cases here.

It is important to note that a full set of period-2^k unstable cycles exists at the critical points. These are the cycles that have appeared and lost their stability during a period-doubling cascade along a particular route in the parameter plane towards a critical point. For Feigenbaum's critical points these cycles are characterized by the universal value of the multiplier $\mu_F = -1.6011913\ldots$. For codimension-2 critical points the behavior of the multipliers for period-2^k cycles depend on the *UD*-code [Kuznetsov *et al.*, 1993b]. Namely, each pattern of K symbols U and D (one period of the code) gives rise to a certain set of K universal multipliers for cycles of period-2^k, $2^{k+1}, \ldots, 2^{k+K}$. (In general, not all of these K numbers are distinct.) Using the *RG* equation solution we obtain precisely the following values of these universal multipliers:

— for tricritical codes, $\ldots UUUU\ldots$ and $\ldots DDDD\ldots$

$$\mu_T = -2.05094049\ldots , \tag{8}$$

— for period-2 code $\ldots UDUD\ldots$

$$\begin{aligned} \mu_1 &= -2.27516954\ldots , \\ \mu_2 &= -2.27516954\ldots , \end{aligned} \tag{9}$$

— for period-3 code $\ldots UUDUUD\ldots$

$$\begin{aligned}\mu_1 &= -2.14347576\ldots,\\ \mu_2 &= -2.25392276\ldots,\\ \mu_3 &= -2.27787495\ldots,\end{aligned} \tag{10}$$

Now we are ready to address the main question of this section: Do the non-Feigenbaum criticality types survive when we use the exact Chua's equations or the exact Poincaré 2D-map instead of the approximate Chua's 1D map?

It seems difficult here (if possible at all) to adopt the search procedure for codimension-2 critical points that was used for 1D maps. So, we have to find another approach. Let us construct artificially a map containing an additional parameter ε; for $\varepsilon = 0$ the map must reduce to Chua's 1D map, and for $\varepsilon = 1$ it has to converge to the exact Poincaré 2D map. Using notations (4) and (5) we may write the new map as

$$X' = (1-\varepsilon)G(X) + \varepsilon G(X), \quad Y' = \varepsilon F(X, Y). \tag{11}$$

Suppose we have found the parameter values α and β for a codimension-2 critical point of Chua's 1D map. So, we know (α, β) for the map (11) at $\varepsilon = 0$. Then we increase ε from 0 to 1 and try to trace the critical point by tuning the control parameters α and β. These parameters are selected permanently to make the main multipliers for sufficiently long period-2^k and 2^{k+1} cycles equal to the corresponding universal values. To be sure of the result, it is desirable to repeat the calculations for larger cycle periods and verify the convergence. Our calculations show that *this procedure works well for codimension-2 critical points except the tricritical ones.*

From a formal point of view, introducing a second dimension in our map (11) means that some perturbation appears in the solution of the RG equation. In general, we have to suppose that all unstable eigenvectors (modes) are present in this perturbation. If we have *two* unstable modes then the perturbation may be compensated by an appropriate shift of two control parameters α and β. In other words, introducing a second dimension leads in this case only to a small displacement of the critical point. In Table 2, we give the parameter values for some critical points of Chua's system. Figure 9 shows their location in the parameter plane.

We can carry out some calculations to demonstrate that the scaling properties of the universality classes intrinsic to bimodal 1D maps really occur at the above critical points of Chua's system.

In Table 2, the values of the main multiplier are presented for cycles of period-2^K at the codimension-2 critical points. For sufficiently large K we see that their behavior coincides well with that expected from the *RG* analysis.

In Fig. 10 portraits of critical attractors are shown for Chua's system at the critical points associated with period-2 and period-3 codes. We demonstrate that the structure of "strips" forming an attractor is reproduced under subsequent magnification by corresponding factors obtained from the *RG* analysis. We believe that the Hausdorff dimensions of these attractors are equal to $D+1$ with $D = 0.643$ and 0.616, respectively (see Kuznetsov *et al.* [1993b] where the results were given for Chua's 1D map).

In Fig. 11, we show an example of self-similar local topography near the codimension-2 critical point having a period-2 code $UDUDUD\ldots$ ($\alpha_C = 3.390136813$, $\beta_C = 4.054379240$). For this example we use the following special scaling coordinates

$$\begin{aligned}\alpha &= \alpha_C + 0.54C_1 + 0.67C_2,\\ \beta &= \beta_C + 0.83C_1 + 1.00C_2\end{aligned} \tag{12}$$

(The coefficients in (12) do not differ notably from that used in Kuznetsov *et al.* [1993b], but the difference in α_C and β_C is essential.) In each of these pictures a critical point is located exactly at the center. A small box enclosing this center is marked and shown on the right side under magnification. The magnification factors are chosen to be equal to the eigenvalues found from the *RG* analysis ($\delta_1 = 35.928\ldots$ and $\delta_2 = 14.595\ldots$). Remarkable reproduction of the topographic patterns under magnification confirms the assumed nature of the observed criticality.

Now, let us consider what is happening with tricritical points. In this case the solution of the linearized *RG* equation gives *three* essential eigenvectors (see Appendix 2). Since we have a bimodal 1D map, any variation of two control parameters induces only perturbations that contain two modes with eigenvalues $\delta_1 = 7.284\ldots$ and $\delta_2 = 2.857\ldots$ [Kuznetsov, 1994]. But introducing a second dimension gives rise also to a third unstable mode that has an eigenvalue $\delta_3 = -4.829\ldots$. It is impossible to compensate for this contribution by varying the parameters of the 1D map: They influence only

Table 2. Codimension-2 critical points and multipliers of cycles in Chua's 1D map and Chua's system.

Code *UDUDUDUDU...*			
Cycle Period	Chua's 1D Map $\alpha = 3.39053346530$ $\beta = 4.05493267746$	Chua's System $\alpha = 3.39013681285$ $\beta = 4.05437923971$	Universal Multipliers from *RG*
2	−2.00625	−2.00619	
4	−2.40316	−2.40306	
8	−2.28483	−2.28479	
16	−2.26394	−2.26396	
32	−2.27732	−2.27732	
64	−2.27538	−2.27537	...
128	−2.27495	−2.27509	...
256	−2.27527	−2.27511	...
512	−2.27480	−2.27555	−2.27516954

Code *UUDUUDUUD...*			
Cycle Period	Chua's 1D Map $\alpha = 3.4725066554$ $\beta = 4.1864354905$	Chua's System $\alpha = 3.47201051860$ $\beta = 4.18571434895$	Universal Multipliers from *RG*
2	−2.11587	−2.11578	
4	−2.18664	−2.18666	
8	−2.17338	−2.17326	
16	−2.24806	−2.24805	...
32	−2.27993	−2.27995	...
64	−2.14337	−2.14338	...
128	−2.25395	−2.25387	−2.25392276
256	−2.27887	−2.27781	−2.27787495
512	−2.14260	−2.14357	−2.14347576

Code *UUUDUUDUUD...*			
Cycle Period	Chua's 1D Map $\alpha = 3.45202980985$ $\beta = 4.15724282857$	Chua's System $\alpha = 3.4514728976$ $\beta = 4.1564292083$	Universal Multipliers from *RG*
2	−2.04008	−2.03986	
4	−2.21220	−2.21175	
8	−2.25811	−2.25853	
16	−2.15145	−2.15193	...
32	−2.25214	−2.25216	...
64	−2.27836	−2.27828	...
128	−2.14349	−2.14348	−2.14347576
256	−2.25385	−2.25381	−2.25392276
512	−2.27683	−2.27665	−2.27787495

Code *UDUUDUUDUU...*			
Cycle Period	Chua's 1D Map $\alpha = 3.38738457711$ $\beta = 4.05035685993$	Chua's System $\alpha = 3.3869901672$ $\beta = 4.0498068716$	Universal Multipliers from *RG*
2	−1.99745	−1.99740	
4	−2.24976	−2.24969	
8	−2.24186	−2.24186	
16	−2.28851	−2.28849	...

Table 2. (*Continued*)

Code *UDUUDUUDUU...*			
Cycle Period	Chua's 1D Map $\alpha = 3.38738457711$ $\beta = 4.05035685993$	Chua's System $\alpha = 3.3869901672$ $\beta = 4.0498068716$	Universal Multipliers from *RG*
32	−2.14179	−2.14179	...
64	−2.25407	−2.25407	...
128	−2.27778	−2.27777	−2.27787495
256	−2.14347	−2.14351	−2.14347576
512	−2.25511	−2.25495	−2.25392276
Code *UDDUDDUDD...*			
Cycle Period	Chua's 1D Map $\alpha = 3.3523870919$ $\beta = 3.9963969715$	Chua's System $\alpha = 3.3520117584$ $\beta = 3.9958795311$	Universal Multipliers from *RG*
2	−1.92006	−1.92000	
4	−2.40030	−2.40012	
8	−2.25962	−2.25966	...
16	−2.13863	−2.13861	...
32	−2.25614	−2.25608	...
64	−2.27788	−2.27763	−2.27787495
128	−2.14351	−2.14255	−2.14347576
256	−2.25312	−2.24978	−2.25392276

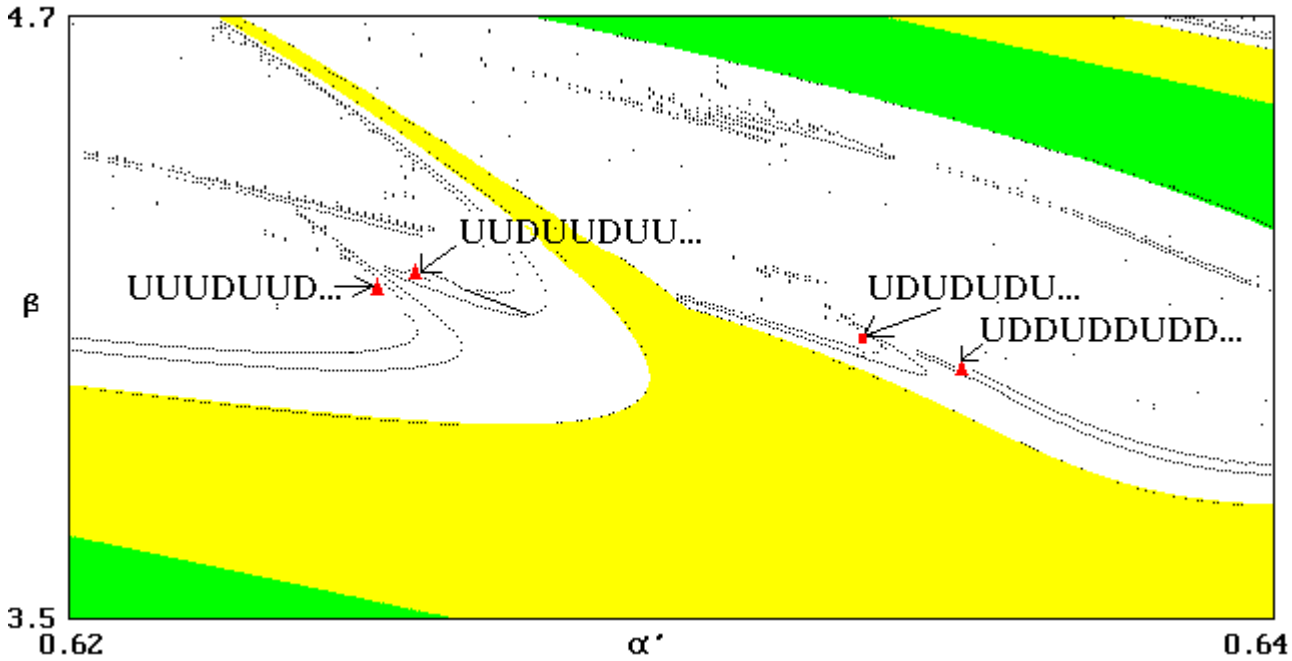

Fig. 9. Sketch of the parameter plane of Chua's system where the location of several codimension-2 critical points is shown. The red square and triangles denote critical points corresponding to *RG* cycles of period-2 and -3, respectively.

the amplitudes of the first and second modes! So, *tricriticality does not survive.* We have to conclude that it does *not* exist in an exact sense in Chua's equations as a codimension-2 phenomenon.

Let us consider next the difference between tricriticality and other codimension-2 types of critical behavior using a rather heuristic argument. Let us suppose that we obtain some definite

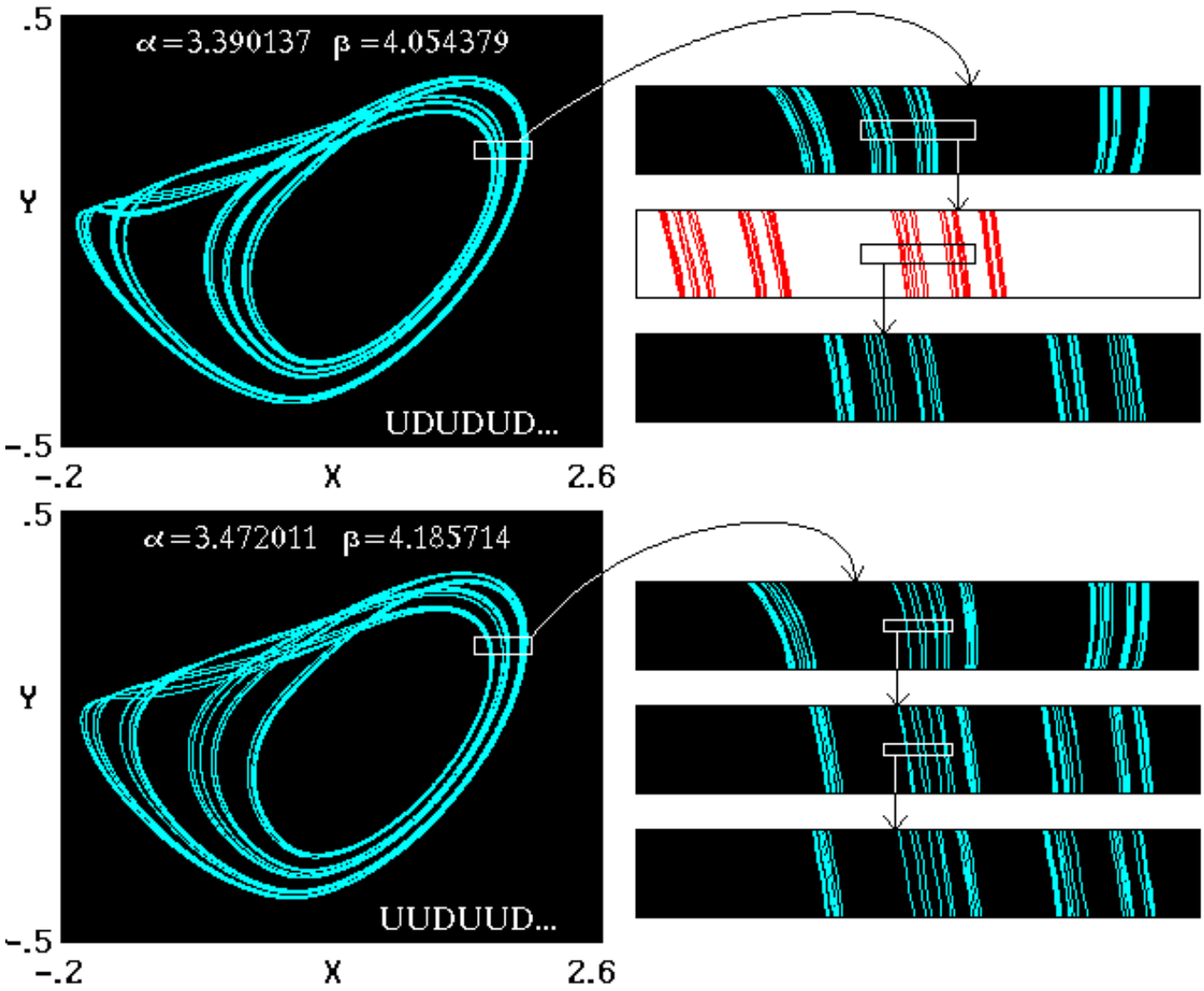

Fig. 10. Critical attractors of Chua's system (2) at the codimension-2 critical points. Self-similarity of the attractor structure is illustrated by showing separately parts of the pictures with increasing resolution, and seen under increasing resolution. The magnification factors $|a|$ are equal to 4.8626... and 8.03026... for (a) and (b), respectively.

codimension-2 critical situation in a 2D map $F : (x, y) \to F(x, y)$. We can define the dynamics over 2^k iterations as a composition of two maps, a p-fold and q-fold iterated maps F^p and F^q, respectively, and the pair (p, q) is the kth term of the sequence given by the rule (7). In the case of a dissipative system it is reasonable to assume that the Jacobian of the map F has an order of magnitude $b < 1$. Then, the Jacobians of the maps F^p and F^q will be of order b^p and b^q, respectively. If both numbers p and q tend to infinity when $k =\to \infty$, both Jacobians will tend to zero. This means that both F^p and F^q will tend to 1D maps. This is precisely the case when the theory of bimodal 1D maps describes adequately the critical behavior of the original system in the asymptotic situation as $k \to \infty$. The above condition is, apparently, valid for all infinite *UD*-codes, *except the tricritical ones.*

On the contrary, in the tricritical case, when we have a repeated symbol U (or D) in the code, the number p (or q) remains constant with increasing k. This means that one of the two maps F^p (or F^q) retains a finite Jacobian $b = b^p$ (or $b = b^q$) and does not reduce to a 1D map when $k \to \infty$. We call this map *a non-1D-component.* In a large-period asymptotic limit the dynamics is described by the composition of the non-1D-component and the 1D map. This composition itself appears to be a 1D map, but in general its extremum *will not be quartic.* (As an example, we may consider a composition of two maps $F : (x, y) \to (x^2 - by, x)$ and $G : (x, y) \to (x^2, x)$. The resulting map

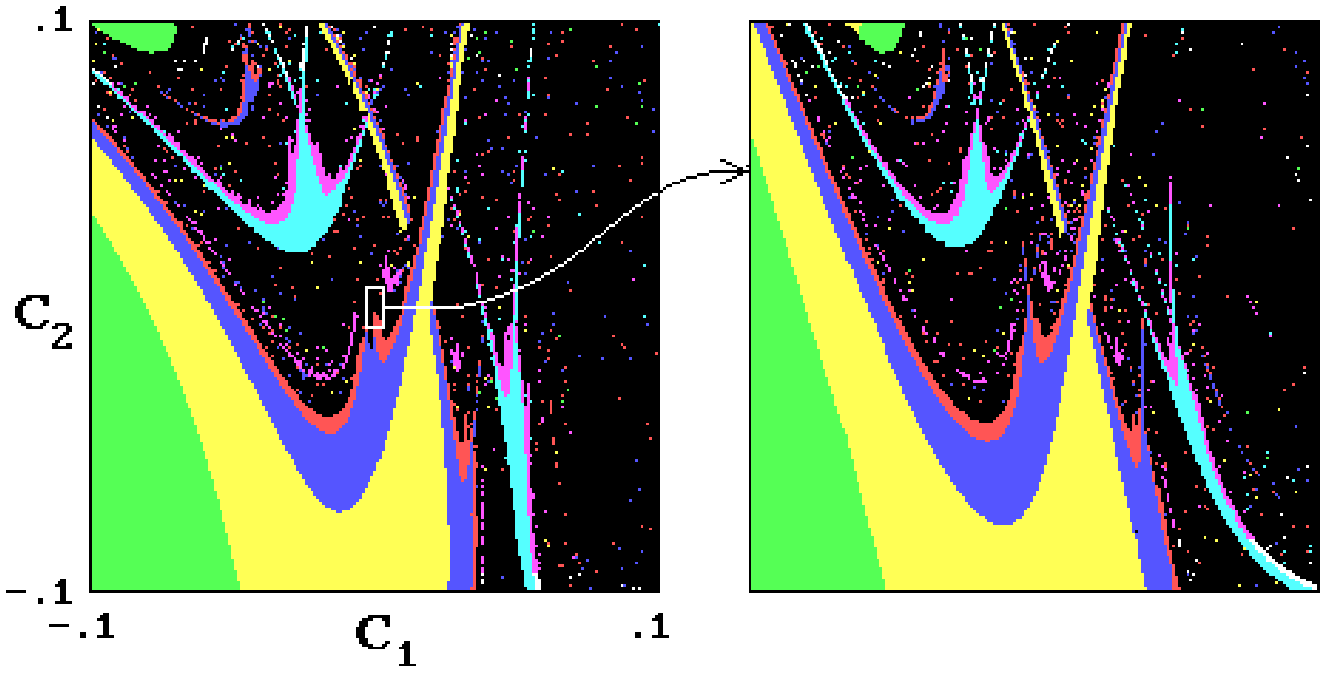

Fig. 11. The universal two-dimensional pattern of the parameter plane topography near the critical point with the period-2 code *UDUDUD*... for Chua's system. The critical point is located exactly at the center of the pictures. Scaling coordinates (C_1, C_2) are used (see text). The picture on the right shows a small box after magnification by $\delta_1 = 35.928\ldots$ and $\delta_2 = 14.595\ldots$ along the horizontal and vertical axes, respectively. For the left picture: green – period $4T$, yellow – $8T$, violet – $16T$, red – $32T$, pink – $12T$, light blue – $24T$, where T is a basic period. For the figure on the right all periods corresponding to the same colors are quadrupled.

$FG : (x, y) \to (x^4 - bx, x)$ is actually 1D, namely $x \to x^4 - bx$. But the quartic extremum, exists only at $b = 0$.)

However, let us consider a tricritical code which has an alternating *UD*-string of r symbols in front of the tail of repeating *U*s (or *D*s). In such a case the Jacobian of the non-1D-component is of the order $b_r = b^{\min(p,q)}$, and for small b decreases with r *very rapidly*. The perturbation of the multiplier for a period-$(p + q)$ cycle due to the presence of the second dimension will be of the same order, as well as the third mode amplitude in the solution of the linearized *RG* equation. During subsequent period-doublings this contribution increases as $b_r(\delta_3)^k$, where $\delta_3 = -4.829\ldots$, and k is the number of doublings. But even for $r = 2$, 3, the initial amplitude may be so small that one observes a *very large* number of period-doubling bifurcations before a notable deviation from tricritical behavior appears. (The intrinsic sequence of period-doublings begins only after the rth bifurcation because the previous iterations are influenced by the initial portion of the UD-code. Features of tricriticality must not be expected at iteration numbers less than 2^r.)

We can estimate the number N, assuming $b_r|\delta_3|^N \cong 1$, so

$$N \cong \frac{-\log b_r}{\log|\delta_3|} \tag{13a}$$

or

$$N \cong \min(p, q)N_o\,, \tag{13b}$$

where $N_o = (-\log b)/(\log|\delta_3|)$ is the characteristic number of the period-doubling bifurcations corresponding to the destruction of the "basic" tricritical situation with the code *UUUUU*.... The mean value of the Jacobian for Chua's system in the parameter area of our interest is $b \cong 3.5 \cdot 10^{-4}$, so $N \cong 5$. Then for some simple tricritical codes we have:

$$UUUUUU\ldots\,, \quad b_r = b\,, \quad N \cong 5\,;$$
$$UDDDDD\ldots\,, \quad b_r = b^3\,, \quad N \cong 15\,;$$
$$UDUUUU\ldots\,, \quad b_r = b^5\,, \quad N \cong 25\,;$$

and so on.

The following calculations may help illustrate the destruction of two-parameter tricriticality. At

first, we try to find such parameter values α and β to make the main multipliers μ_k and μ_{k+1} for cycles of period 2^k and 2^{k+1} equal to the universal tricritical constant $\mu_T = -2.0574\ldots$. Then at the same point we evaluate also the multiplier μ_{k+2} for the period-2^{k+2} cycle. The procedure is repeated for increasing k to observe the behavior of the calculated μ_{k+2}. Only for a 1D map we find actually that these multipliers converge to the same μ_T (see Table 3). *For 2D-maps an increasing deviation is observed from this value, alternately up and down.* Certainly, it reveals a contribution of the third mode (with negative eigenvalues). Note that the order of N was evaluated correctly.

However, in physical experiments it would be unrealistic to speak about observations of more than 4–6 period-doubling bifurcations. So, from a practical point of view, the behavior of being observed may not be distinguishable from tricriticality (except maybe the code *UUUU...*). Moreover, according to our evaluation, it may be difficult to detect the destruction of tricriticality even in precise computer calculations. Tricritical behavior appears in these cases as *intermediate asymptotics.* We call such behavior *pseudo-tricritical.* Note that the parameter values for this situation may be defined in principle only with a finite accuracy. Nevertheless, this precision may be very high. With this reservation we can speak of *pseudo-tricritical points.* (In a pure sense they are not points: One has to imagine rather a very small localized area in the parameter plane and deal with such timescales that do not resolve the interior structure of this area.) In Fig. 12 we show an example of a pseudo-tricritical attractor for Chua's system at the point $\alpha = 3.382469913$, $\beta = 4.043044760$. We demonstrate the fine structure of the attractor by showing a number of pictures with increasing resolution. The factor of magnification is taken equal to the tricritical scaling constant 1.6903.... We conjecture

Table 3. Multipliers of cycles: Convergence at tricritical points of Chua's 1D map and divergence from Chua's system.

Code *UUUUUUUUU...*						
	Chua's 1D Map			Chua's System		
k	α	β	μ_{k+2}	α	β	μ_{k+2}
2	3.430079828	4.124595158	−1.52642	3.429592279	4.123886268	−1.50571
3	3.426890291	4.119881278	−1.91796	3.426291905	4.119008902	−2.00741
4	3.426510760	4.119315946	−2.01283	3.426165396	4.118820467	−1.57859
5	3.426468878	4.119253404	−2.04010	3.425686367	4.118105199	−3.64479
6	3.426464561	4.119246952	−2.04775			
Code *UDDDDDDDD...*						
	Chua's 1D Map			Chua's System		
k	α	β	μ_{k+2}	α	β	μ_{k+2}
3	3.326462742	3.957169248	−1.40226	3.326102885	3.956677005	−1.40282
4	3.324849419	3.954734357	−2.17048	3.324491683	3.954245421	−2.17045
5	3.324978268	3.954928594	−2.01965	3.324620425	3.954439488	−2.01966
6	3.324966741	3.954911224	−2.05821	3.324608908	3.954422134	−2.05821
7	3.324967612	3.954912537	−2.05602	3.324609856	3.954423563	−2.04923
Code *UDUUUUUUU...*						
	Chua's 1D Map			Chua's System		
k	α	β	μ_{k+2}	α	β	μ_{k+2}
3	3.383031029	4.043842842	−1.90629	3.382638800	4.043296428	−1.90643
4	3.382880433	4.043618446	−2.01094	3.382488416	4.043072356	−2.01079
5	3.382859737	4.043587442	−2.06470	3.382467651	4.043041250	−2.06471
6	3.382862527	4.043591627	−2.04485	3.382470442	4.043045437	−2.04479
7	3.382862111	4.043591002	−2.04741	3.382469991	4.043044761	−2.04738

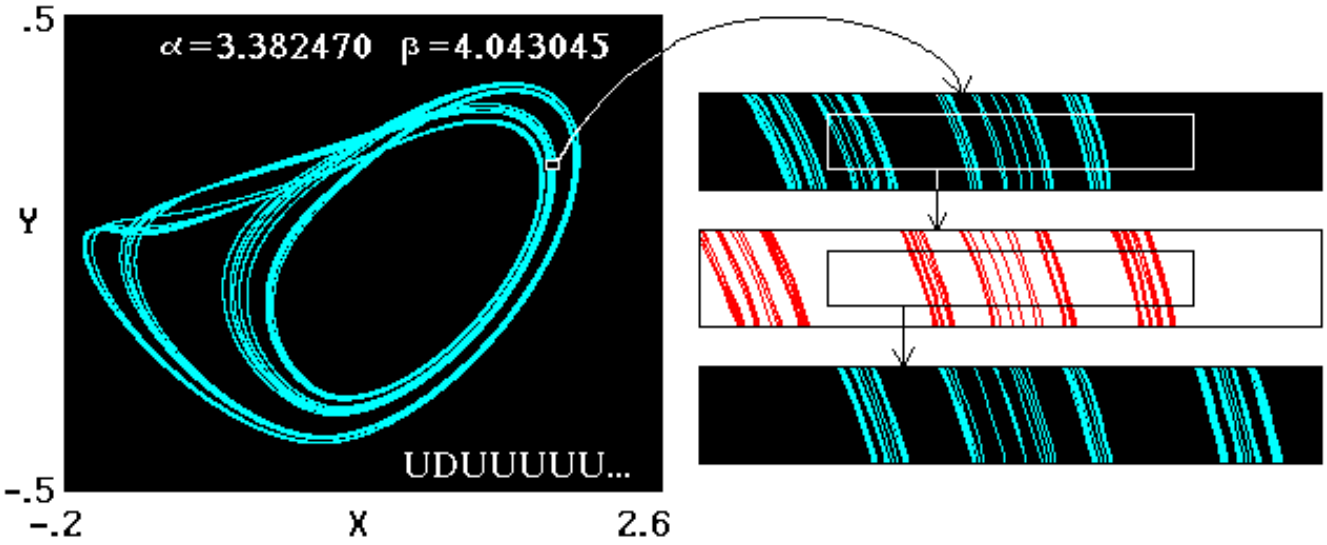

Fig. 12. Attractor of Chua's system at a pseudo-tricritical point. Self-similarity of the attractor structure is valid only up to some finite level of resolution that is not achieved in the computations. Magnification factor $|a| = 1.6903\ldots$.

that this attractor has a self-similar structure only up to a finite level of resolution which is not attained in our computations.

The above situation is more of a rule than an exception in the world of fractals: Self-similarity appears always in a restricted interval of scales. In any case we have to emphasize the difference from Feigenbaum's criticality: The destruction of scaling invariance in small scales appears to be due to pure dynamical reasons.

4. Critical Behavior in a System of Two Chua's Circuits with a Unidirectional Coupling

In previous works (see Kuznetsov *et al.* [1991, 1993a]) transition to chaos was investigated in a system of two logistic maps with an unidirectional coupling:

$$x_{n+1} = 1 - \lambda x_n^2\,, \quad y_{n+1} = 1 - Ay_n^2 - Bx_n^2\,, \quad (14)$$

where x and y are dynamical variables, λ and A are control parameters for the first and second subsystems, respectively, and B is the coupling constant, assumed to satisfy $0 \leqslant B \leqslant \lambda$. In this paper we shall deal with two interesting critical situations in a system with unidirectional coupling. The first one is *the double Feigenbaum point DF* and the second is *the bicritical point B*.

For zero coupling ($B = 0$) and $\lambda = A = \lambda_C = 1.401155\ldots$ both subsystems exhibit Feigenbaum's criticality. However, a question of interest is how does the topography of the parameter space (λ, A, B) look near this double Feigenbaum point and what are its scaling properties.

The bicritical type of behavior appears when one tunes parameters λ and A to reach a threshold of chaos in both subsystems while keeping the coupling constant. For example, taking $B = 0.375$ we have found that the bicritical point is located at $\lambda = 1.401155\ldots$, $A = 1.124981403$ (Kuznetsov *et al.* [1991]). A remarkable fact is that the scaling properties of bicriticality do not depend on the particular value of coupling. They are universal and relate to a definite fixed point of *RG* equations that are a generalization of (6) for two systems with a unidirectional coupling.

In Appendix 3, we describe briefly the *RG* analysis for *DF* and *B* types of critical behavior.

Now let us discuss in some detail the particular nature of coupling in Eqs. (14). We can rewrite them in an equivalent form

$$\begin{aligned} x_{n+1} &= 1 - \lambda x_n^2\,, \\ y_{n+1} &= 1 - A' y_n^2 - B(x_n^2 - y_n^2)\,, \end{aligned} \quad (15)$$

where $A' = A + B$. It is clear that for $A' = \lambda$ the system has an invariant set $x = y$. Let us consider the evolution of small perturbations near the invariant set. For the perturbation $\tilde{x}$ of the first subsystem we have

$$\tilde{x}_{n+1} = -2\lambda x_n \tilde{x}_n\,. \quad (16)$$

For the perturbation $\tilde{y} = y - x$, shifting the second subsystem from the invariant set, we obtain for $A' = \lambda$

$$\tilde{y}_{n+1} = -2(\lambda - B)x_n\tilde{y}_n\,. \tag{17}$$

Observe that the ratio $\tilde{y}/\tilde{x}$ decays as $(1-B/\lambda)^n$. We see that the influence of coupling is a tendency to equalize the instant states of both subsystems. For this reason we call such couplings dissipative (see Pikovsky [1984], Kuznetsov & Pikovsky [1986], Kuznetsov [1985]).

How could we organize analogous couplings for two systems governed by differential equations, say

$$\frac{dx}{dt} = f(x, y, z)\,, \quad \frac{dy}{dt} = g(x, y, z)\,, \quad \frac{dz}{dt} = h(x, y, z)\,? \tag{18}$$

Let us add to all the equations of the second subsystem similar dissipative-difference terms:

$$\begin{aligned}
\frac{dx_1}{dt} &= f(x_1, y_1, z_1)\,,\\
\frac{dy_1}{dt} &= g(x_1, y_1, z_1)\,,\\
\frac{dz_1}{dt} &= h(x_1, y_1, z_1)\,,\\
\frac{dx_2}{dt} &= f(x_2, y_2, z_2) + \varepsilon(x_2 - x_1)\,,\\
\frac{dy_2}{dt} &= g(x_2, y_2, z_2) + \varepsilon(y_2 - y_1)\,,\\
\frac{dz_2}{dt} &= h(x_2, y_2, z_2) + \varepsilon(z_2 - z_1)\,,
\end{aligned} \tag{19}$$

In some sense the properties of these equations are very similar to those of the model maps (14). Again we have an invariant set in the state space, that is $x_1 = x_2$, $y_1 = y_2$, $z_1 = z_2$. For a small perturbation of the first subsystem $\tilde{x} = (\tilde{x}_1, \tilde{y}_1, \tilde{z}_1)$ we obtain

$$\frac{d\tilde{x}}{dt} = \hat{M}(x)\tilde{x}\,, \tag{20}$$

where $\hat{M}$ is a matrix of partial derivatives of the functions f, g, h. In a similar way, for perturbations of the second subsystem near the invariant set, $\tilde{\mathbf{y}} = (x_2 - x_1, y_2 - y_1, z_2 - z_1)$ we find

$$\frac{d\tilde{\mathbf{y}}}{dt} = \hat{\mathbf{M}}(\mathbf{x})\tilde{\mathbf{y}} + \varepsilon\tilde{\mathbf{y}}\,. \tag{21}$$

Comparing Eqs. (20) and (21) one can see that $\tilde{\mathbf{y}}(t) = \tilde{\mathbf{x}}(t)\exp(-\varepsilon t)$. So, the coupling forces the non-uniform perturbations to decay more rapidly. This is just our basic criterion for dissipative coupling. If the individual subsystem (18) exhibits a period-doubling transition to chaos we may expect in the coupled systems (19) the same types of behavior as in the coupled maps (14).

Now let us choose Chua's circuit as an elementary cell and add coupling according to our prescription:

$$\begin{aligned}
\frac{dx_1}{dt} &= \alpha_1(y_1 - h(x_1))\,,\\
\frac{dy_1}{dt} &= x_1 - y_1 + z_1\,,\\
\frac{dz_1}{dt} &= -\beta_1 y_1\,,\\
\frac{dx_2}{dt} &= \alpha_2(y_2 - h(x_2)) + \varepsilon(x_2 - x_1)\,,\\
\frac{dy_2}{dt} &= x_2 - y_2 + z_2 + \varepsilon(y_2 - y_1)\,,\\
\frac{dz_2}{dt} &= -\beta_2 y_2 + \varepsilon(z_2 - z_1)\,.
\end{aligned} \tag{22}$$

In practice the unidirectional coupling in an electronic system can be easily implemented via an operational amplifier in the connection circuit. (See experimental works of Bezruchko *et al.* [1986]; Anishchenko *et al.* [1986]; Johnson *et al.* [1995]). We believe that the expected universal properties of critical behavior will not depend essentially on the particular method of coupling.

Now we turn to an investigation of the critical behavior in Eqs. (22). Choosing arbitrary $\beta = 10$ we find a sequence of period-doubling bifurcation values α_k in an individual subsystem (see the left column of Table 5). The Feigenbaum critical point is located at $\alpha_C = 6.542725993$. So, the parameter values $\alpha_1 = \alpha_2 = \alpha_C$ and $\varepsilon = 0$ correspond to the double Feigenbaum point for $\beta_1 = \beta_2 = 10$. According to results of the *RG* analysis (Appendix 3) we must observe similar dynamical regimes in a neighborhood of the *DF* point in the 3D parameter space $(\alpha_1, \alpha_2, \varepsilon)$ if we renormalize $\alpha_1 - \alpha_C$ and $\alpha_2 - \alpha_C$ by a factor equal to $\delta_F = 4.6692\ldots$, and ε by a factor equal to 2. In Fig. 13, we show a cross section of the parameter space by a plane $\alpha_2 = \alpha_C$. Observe

that the topography of this parameter plane near the *DF* point is really reproduced well under the above rescaling.

Now we turn to a procedure for searching a bicritical point. For the same $\beta_1 = \beta_2 = 10$ we take arbitrarily a constant coupling parameter $\varepsilon = 0.2$ and consider the parameter plane (α_1, α_2) (Fig. 14). Evidently, period-doubling bifurcations in the first system occur at the vertical straight lines $\alpha_1 = \alpha_{1k}$. These lines correspond to a loss of stability of period-2^k cycles in the first subsystem. There is one multiplier μ_1 equal to (-1) that relates to the perturbations of the first subsystem. At the same time for small α_2 the second subsystem exhibits a forced response with the same period. This regime is stable with respect to perturbations of the second subsystem, since the corresponding multiplier μ_2 has an absolute value less than unity. Let us move up in the parameter plane along one of the lines $\alpha_1 = \alpha_{1k}$: We increase α_2 and trace the multiplier μ_2. At some point we observe that μ_2 also becomes equal to -1. This means that we achieve a threshold of instability in the second subsystem. This point where both $\mu_1 = -1$ and $\mu_2 = -1$ we call *a terminal point*. Taking another bifurcation number $k + 1$ we obtain the next terminal point, and

Table 4. Terminal point sequence converging to the bicritical point in two Chua's systems with a unidirectional coupling (Eqs. (22), $\beta_{1,2} = 10$, $\varepsilon = 0.2$).

N	α_1	α_2
2	6.503682576	6.626251829
4	6.534427453	6.642445754
8	6.540951444	6.645142689
16	6.542345864	6.646282931
32	6.542644382	6.646585909
64	6.542708309	6.646734076
128	6.542722000	6.646774157
256	6.542724932	6.646795959
	6.542725993	6.64680875

Table 5. Main multipliers of period-2^k cycles at the bicritical point of two Chua's systems with a unidirectional coupling: $\alpha_1 = 6.542725993307$, $\alpha_2 = 6.64680875$, $\beta_{1,2} = 10$, $\varepsilon = 0.2$.

2	−1.6010262	−1.17244707
4	−1.6011441	−1.15905841
8	−1.6012009	−1.17877276
16	−1.6011899	−1.17302502
32	−1.6011915	−1.18246344
64	−1.6011913	−1.17417212
128	−1.6011912	−1.18249718
256	−1.6011909	−1.17602951
512	−1.6011893	−1.18288097
1024	−1.6011816	−1.17888254

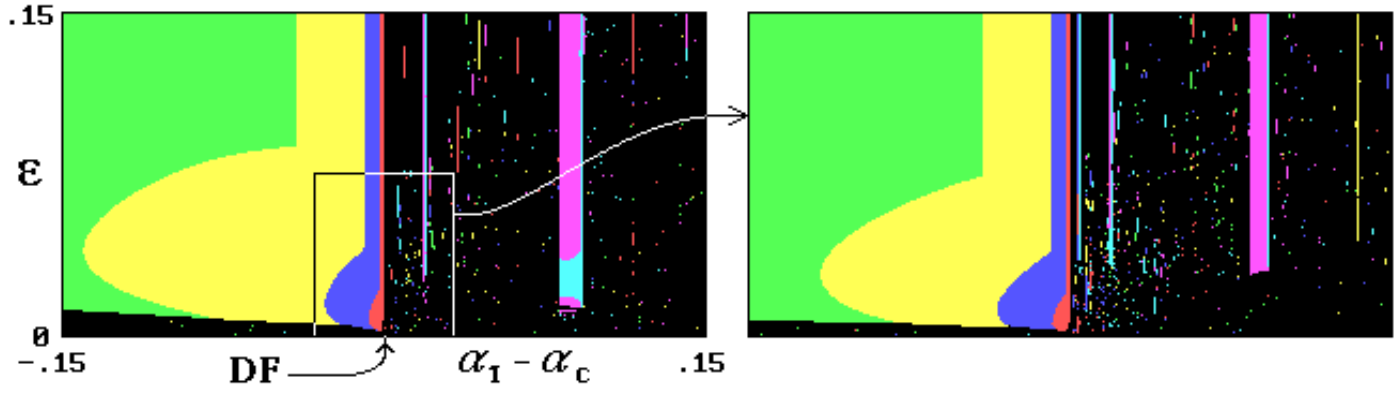

Fig. 13. The universal pattern of the parameter space topography in the cross section by coordinate plane $\alpha_2 = \alpha_C = 6.542725\ldots$ in the neighborhood of a double Feigenbaum's point in two of Chua's system with a unidirectional coupling, $\beta_1 = \beta_2 = 10$. The horizontal axis corresponds to the control parameter of the first subsystem and the vertical axis corresponds to the coupling parameter. The picture on the right shows a small box after magnification by $\delta_1 = 4.6692\ldots$ and $\delta_3 = 2\ldots$ along the horizontal and vertical axes, respectively. For the left picture: green – period $2T$, yellow – $4T$, violet – $8T$, red – $16T$, pink – $6T$, light blue – $12T$, where T is a basic period. For the picture on the right all periods corresponding to the same colors are doubled.

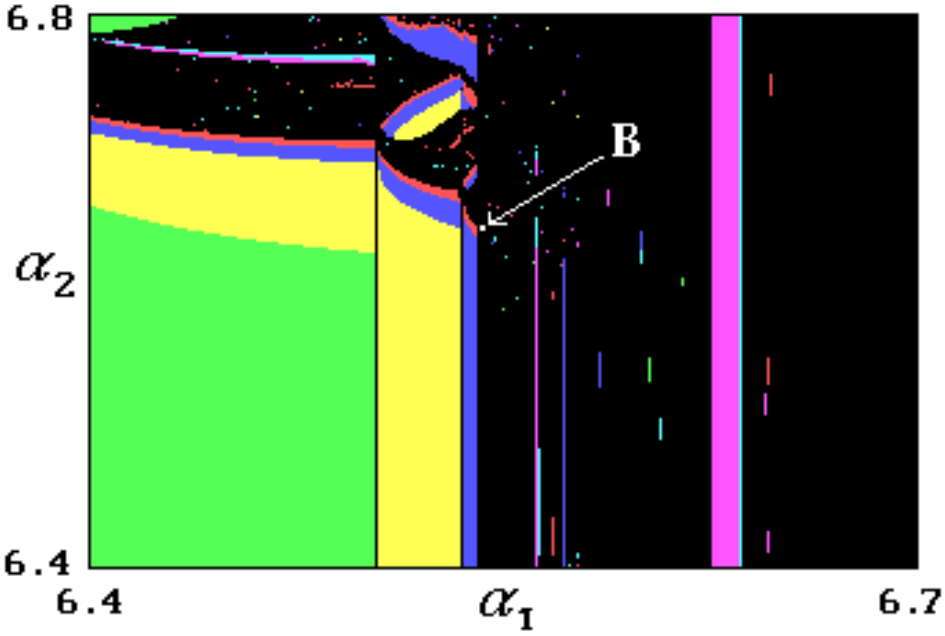

Fig. 14. Parameter plane for two Chua's systems with a unidirectional coupling, $\beta_1 = \beta_2 = 10$, $\varepsilon = 0.2$. The horizontal and vertical axes correspond to control parameters of two subsystems, α_1 and α_2, respectively. The location of bicritical point B is shown.

so on. Coordinates of the terminal points in the parameter plane are listed in Table 4 and clearly demonstrate convergence. Evaluating the limit of this sequence we find the bicritical point

$$\alpha_1 = \alpha_{1C} = 6.542725993\,,$$
$$\alpha_2 = \alpha_{2C} = 6.6468087\,, \quad (\text{for } \varepsilon = 0.2,\ \beta_{1,2} = 10)\,.$$

Now we may produce numerical calculations aimed at illustrating the scaling properties of the bicritical behavior. At the bicritical point the cycles of period 2^k must have asymptotically universal multipliers $\mu_1 = -1.60119\ldots$ and $\mu_2 = -1.178855$ [Kuznetsov *et al.*, 1991]. In Table 5, we present data for the system (22) at the bicritical point. One can see that the multipliers really show a tendency to converge to the above universal values.

In Fig. 15 the phase portraits are shown for the bicritical attractor. The figures (a) and (b) relate to the first and the second subsystem, respectively. It is interesting to compare their scaling properties. In the first plot, the Cantor-like structure reproduces itself under scale change with the Feigenbaum's scaling factor $a_F = -2.5029\ldots$ while for the second subsystem the special bicritical factor $b = -1.505318\ldots$ must be used.

In Fig. 16, a plot is shown for the largest Lyapunov exponent of the second subsystem Λ versus the control parameter α_2 while the first subsystem is kept at Feigenbaum's critical point $\alpha_1 = \alpha_{1C}$. The Lyapunov exponent is negative for small α_2 and starts to take positive values for α_2 larger than α_{2C}. Hence the bicritical point corresponds precisely to the threshold of chaos both in the first and second subsystems. Scaling properties of the Lyapunov exponent are illustrated by comparison of the initial plot with its own magnified parts. For the α_2 coordinate axis the magnification factor is taken to be equal to the eigenvalue $\delta_2 = 2.3927\ldots$ known from the RG analysis (Appendix 3). For the Λ axis, the scaling factor is 2 (a ratio of timescales for similar regimes).

Figure 17 shows a part of the parameter plane (α_1, α_2) near the bicritical point. This picture also demonstrates scaling and reproduces itself under magnification by the factors $\delta_1 = 4.6692\ldots$ and $\delta_2 = 2.3927\ldots$ for the axes α_1 and α_2, respectively.

5. Conclusion

The idea that multi-dimensional dissipative nonlinear systems must exhibit the same universal features as 1D maps at the onset of chaos is accepted as a sort of self-evident thing after the works of Feigenbaum [1978, 1979], Collet *et al.* [1981] and others. However, for other types of multi-parameter

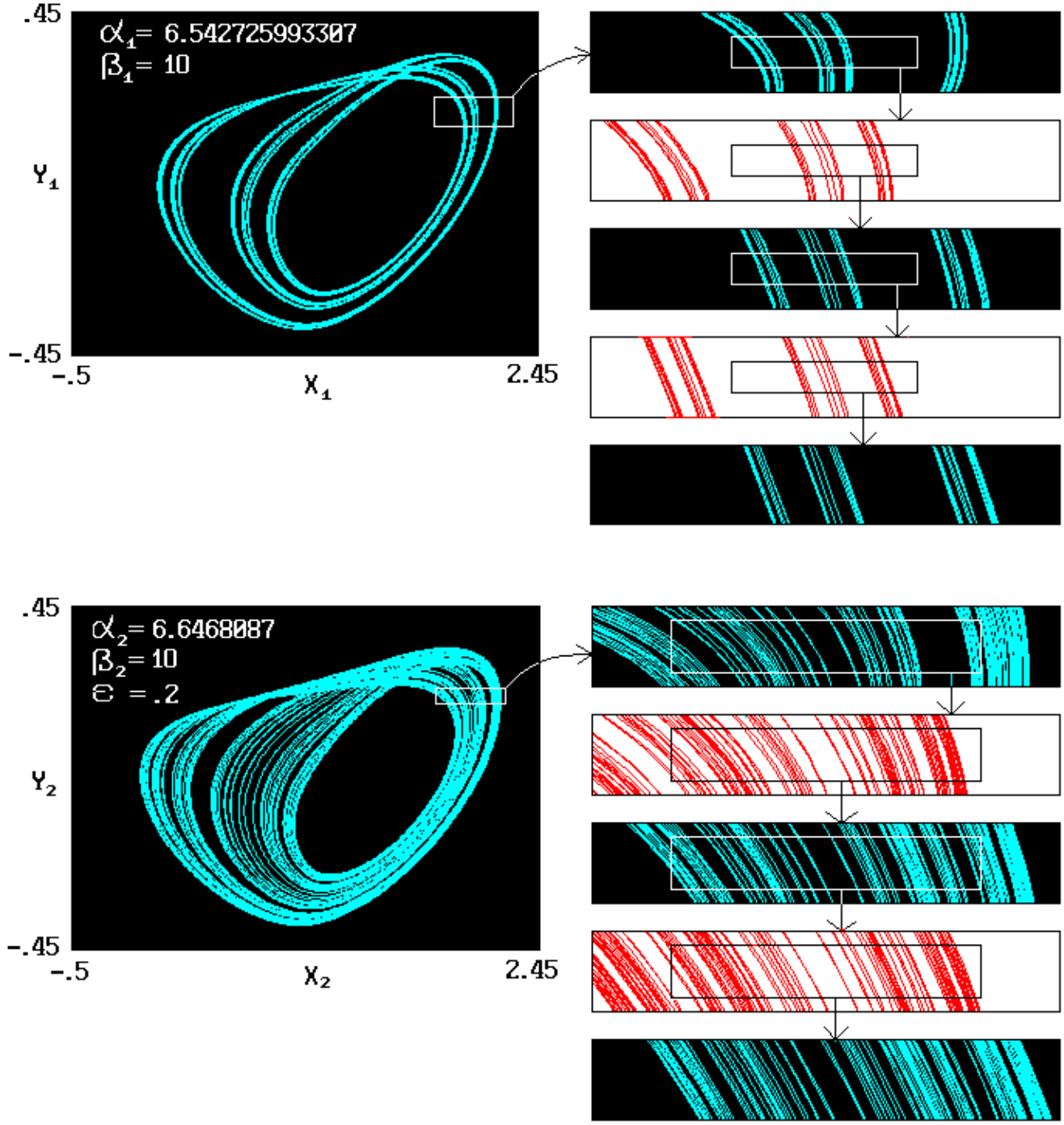

Fig. 15. Attractor portraits for the first (a) and the second (b) subsystems at the bicritical point. Self-similarity of the attractor structure is illustrated by showing separately parts of the pictures with increasing resolution. The magnification factors are equal to $|a| = 2.5029\ldots$ and $|b| = 1.5053\ldots$, respectively. The patterns of strips are repeated at each second step of magnification.

period-doubling criticality, the question is found to be more complicated and subtle. In particular, tricritical behavior easily observable in bimodal 1D maps does not survive as a codimension-2 phenomenon in more general systems. Nevertheless, we have shown that the tricriticality may be considered as a realistic kind of behavior. Indeed, in many cases the departure from tricritical scaling would appear in such subtle details of long-period dynamics that it is impossible to observe it in any real experiment, or even in straightforward computer calculations.

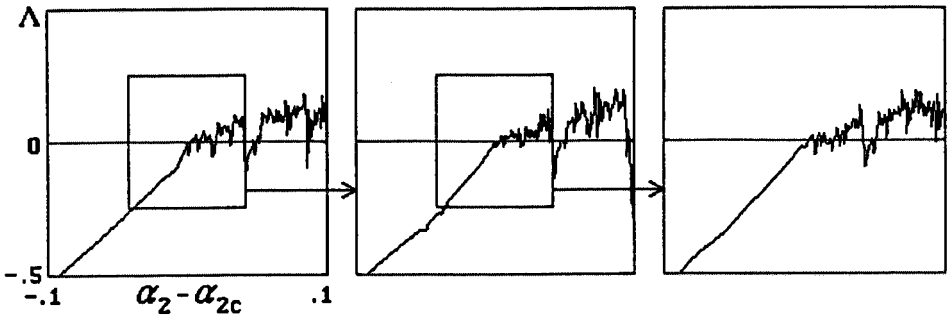

Fig. 16. The Lyapunov exponent for the second subsystem versus its control parameter α_2 for $\alpha_1 = \alpha_C = 6.542725\ldots$, $\beta_1 = \beta_2 = 10$, $\varepsilon = 0.2$. The next figures present the magnified parts of the first one inside the rectangles shown. The magnification factors are equal to $\delta_2 = 2.3927$ for the horizontal axis and 2 for vertical axis.

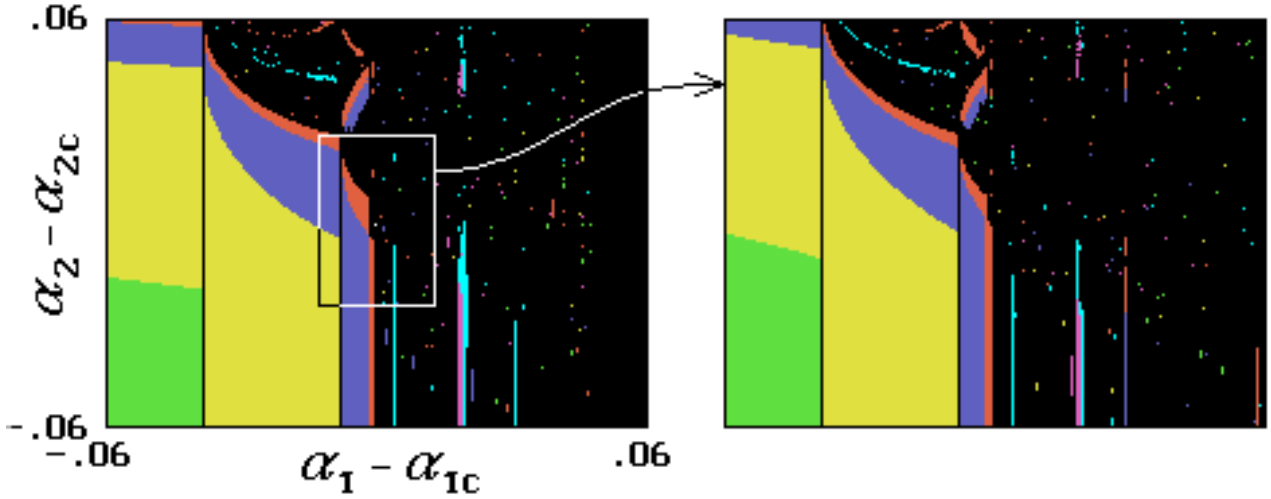

Fig. 17. The universal pattern of two-dimensional topography in the parameter plane in the neighborhood of the bicritical point $\alpha_{1C} = 6.542725\ldots$, $\alpha_{2C} = 6.646808\ldots$ for two Chua's systems with a unidirectional coupling, $\beta_1 = \beta_2 = 10$, $\varepsilon = 0.2$. The bicritical point is located exactly at the center of the pictures. The picture on the right shows a small box after magnification by $\delta_1 = 4.6692\ldots$ and $\delta_3 = 2.3927\ldots$ along the horizontal and vertical axes, respectively. For the left picture: green – period $2T$, yellow – $4T$, violet – $8T$, red – $16T$, pink – $6T$, light blue – $12T$, where T is a basic period. For the picture on the right all periods corresponding to the same colors are doubled.

We have presented in this paper numerical evidence of several non-Feigenbaum period-doubling critical situations in Chua's system and its higher-dimensional version, namely two cells with a unidirectional coupling.

In conclusion we should emphasize one important general concept of the *critical attractor*. We can see now that critical attractors represent a rather broad and interesting class of dynamical objects. The well-known Feigenbaum's attractor at the limit point of an ordinary period-doubling cascade is only one member of this family. Figures 10 and 15 show some other representatives. All of them have a similar Cantor-like structure but these structures have different quantitative characteristics.

It is well known that strange attractors corresponding to developed chaos also have a fractal nature. We note that the features of critical attractors are essentially distinct. First, their fractal structure in the Poincaré section is longitudinal rather than transversal (as for strange attractors). Second, the time scale multiplied by a power of 2 is responsible for each new level of the fractal structure. For strange attractors a new level usually appears each time the trajectory goes around the attractor, i.e., at the same characteristic period. For critical attractors the known Kaplan–Yorke formula is not valid. Fractal dimension is universal for a certain type of criticality and relates to the nature of the

RG equation solution, and not to the spectrum of the Lyapunov exponents.

Acknowledgments

The work was supported in part by a NATO Linkage High Technology grant number HTECH.L6930749, and by grant number 95-02-05818 of the Russian Fund of Fundamental Research.

References

Anishchenko, V. S., Aranson, I. S., Postnov, D. E. & Rabinovich, M. I. [1986] "Spatial synchronization and bifurcation of the chaos development in a chain of connected generators," *Sov. Phys. Dokl.* **31**(2), 169–171.

Bezruchko, B. P., Gulyaev, Yu. V., Kuznetsov, S. P. & Seleznev, E. P. [1986] "New type of critical behavior in coupled systems at the transition to chaos," *Sov. Phys. Dokl.* **31**(3), 258–260.

Carcasses, J., Mira, C., Bosh, M., Simo, C. & Tatjer, J. C. [1991] "Crossroad area — spring area transition. Parameter plane representation," *Int. J. Bifurcation and Chaos* **1**, 183–196.

Chang, S. J., Wortis, M. & Wright, J. A. [1981] "Iteration properties of a one-dimensional quartic map. Critical lines and tricritical behavior," *Phys. Rev.* **A24**, 2669–2684.

Collet, P., Eckmann, J.-P. & Koch, H. [1981] "Period doubling bifurcations for families of maps on R^n," *J. Stat. Phys.* **25**, 1–14.

Chua, L. O., Komuro, M. & Matsumoto, T. [1986] "The double scroll family. Parts I and II," *IEEE Trans. Circuits and Systems* **CAS-33**, 1072–1118.

Eckmann, J.-P., Koch, H. & Wittwer, P. [1982] "Existence of a fixed point of the doubling transformation for area-preserving maps of the plane," *Phys. Rev.* **A26**(1), 720–722.

Feigenbaum, M. J. [1978] "Quantitative universality for a class of nonlinear transformations," *J. Stat. Phys.* **19**, 25–52.

Feigenbaum, M. J. [1979] "The universal metric properties of nonlinear transformations," *J. Stat. Phys.* **21**, 669–706.

Fraser, S. & Kapral, R. [1984] "Universal vector scaling in one-dimensional maps," *Phys. Rev.* **A25**, 3223–3233.

Gambaudo, J. M., Los, J. E. & Tresser, G. [1987] "A horseshoe for the doubling operator topological dynamics for metric universality," *Phys. Lett.* **A123**, 60–64.

Genot, M. [1993] "Application of 1D Chua's map from Chua's circuit: A pictorial guide," *J. of Circuits, Systems and Computers* **3**(2), 431–440.

Halsey, T. S., Jensen, M. H., Kadanoff, L. P., Procaccia, I. & Shraiman, B. I. [1986] "Fractal measures and their singularities," *Phys. Rev.* **A33**, 1141–1151.

Helleman, R. H. G. [1980] "Self-generated chaotic behavior in nonlinear mechanics," in *Fundamental Problems in Statistical Mechanics*, eds. Cohen, E. G. D. *et al.*, vol. 5 (North-Holl. Publ., Amsterdam).

Johnson, G. A., Locher, M. & Hunt E. R. [1995] "Stabilized spatiotemporal waves in a convectively unstable open flow system: Coupled diode resonators," *Phys. Rev.* **E51**, R1625–R1628.

Komuro, M., Tokunaga, R., Matsumoto, T., Chua, L. O. & Hotta, A. [1991] "Global bifurcation analysis of the double scroll circuit," *Int. J. Bifurcation and Chaos* **1**, 139–182.

Kuznetsov, A. P., Kuznetsov, S. P. & Sataev, I. R. [1991] "Bicritical dynamics of period-doubling systems with unidirectional coupling," *Int. J. Bifurcation and Chaos* **1**, 839–848.

Kuznetsov, A. P., Kuznetsov, S. P. & Sataev, I.R. [1993a] "Variety of types of critical behavior and multistability in period-doubling systems with aunidirectional coupling near the onset of chaos," *Int. J. Bifurcation and Chaos* **3**, 139–152.

Kuznetsov, A. P., Kuznetsov, S. P., Sataev, I. R. & Chua, L. O. [1993b] "Two-parameter study of transition to chaos in Chua's circuit: Renormalization group, universality and scaling," *Int. J. Bifurcation and Chaos* **3**, 943–962.

Kuznetsov, A. P., Kuznetsov, S. P. & Sataev, I. R. [1994a] "From bimodal one-dimensional maps to Henon-like two-dimensional maps: Does quantitative universality survive?," *Phys. Lett.* **A184**, 413–421.

Kuznetsov, A. P., Kuznetsov, S. P. & Sataev, I. R. [1994b] "Three-parameter scaling for one-dimensional maps," *Phys. Lett.* **A189**, 367–373.

Kuznetsov, S. P. [1985] "Universality and scaling in behavior of coupled Feigenbaum's systems," *Izvestija vys. uch. zav. Radiofizika* **28**(8), 991–1007.

Kuznetsov, S. P. & Pikovsky, A. S. [1986] "Universality and scaling of period-doubling bifurcations in a dissipative distributed medium," *Physica* **D19**, 384–396.

Kuznetsov, S. P. & Sataev, I. R. [1992] "New types of critical dynamics for two-dimensional maps," *Phys. Lett.* **A162**, 236–242.

Kuznetsov, S. P. [1994] "Tricriticality in two-dimensional maps," *Phys. Lett.* **A169**, 438–444.

Lichtenberg, A. J. & Lieberman, M. A. [1982] *Regular and Stochastic Motion* (Springer, Heidelberg-New York).

MacKay, R. S. & van Zeijts, J. B. J. [1988] "Period-doubling for bimodal map: A horseshoe for a renormalization group operator," *Nonlinearity* **1**(1), 253–277.

Madan, R. N., ed. [1993] *Chua's Circuit: A Paradigm for Chaos* (World Scientific, Singapore).

Pikovsky, A. S. [1984] "On the interaction of strange attractors," *Z. Phys.* **B55**, 149–154.

Appendix 1
Poincaré Map for Chua's Circuit

Constructions for obtaining the Poincaré 2D map have been implemented as a corresponding computer procedure. It is based on analytical integration of Eqs. (2). It is possible because the equations are piecewise-linear; so we avoid any numerical techniques, like Runge–Kutta. The solutions may be found easily for each domain of linearity, and the only problem to be solved numerically is to find the intersections of an orbit with the boundary planes.

We consider here only two domains of linearity, $\mathbf{D}_1$ ($x > 1$) and $\mathbf{D}_0$ ($|x| < 1$). It is sufficient because of the obvious symmetry property: Equations (2) are invariant under the transformation $x \to -x$, $y \to -y$, $z \to -z$. Constructing the map in the case when an orbit visits all three domains is still straightforward, but an interpretation is much more complicated. In this paper we are concerned only with the situation where an orbit visits only two domains. It corresponds to the Rossler-type attractor of Chua's circuit.

A.1. Preliminary Definitions

(a) Stationary points for domains $\mathbf{D}_0$ and $\mathbf{D}_1$ are

$$\mathbf{X}_{D0}^{C} = \{0, 0, 0\} \quad \text{and} \quad \mathbf{X}_{D1}^{c} = \{\mathbf{k}, 0, -\mathbf{k}\} \tag{A1.1}$$

where $\mathbf{k} = (\mathbf{b} - \mathbf{a})/(\mathbf{b} + 1)$.

(b) Vector field matrices for $\mathbf{D}_0$ and $\mathbf{D}_1$ domains are

$$\mathbf{C}_0 = \begin{bmatrix} -\alpha(1+\mathbf{a}) & \alpha & 0 \\ 1 & -1 & 1 \\ 0 & -\beta & 0 \end{bmatrix} \quad \text{and} \quad \mathbf{C}_1 = \begin{bmatrix} -\alpha(1+\mathbf{b}) & \alpha & 0 \\ 1 & -1 & 1 \\ 0 & -\beta & 0 \end{bmatrix}. \tag{A1.2}$$

Eigenvalues of these matrices are obtained from solving the characteristic equations

$$x^3 + [(1+a)\alpha + 1]x^2 + (\alpha a + \beta)x + (1+a)\alpha\beta = 0 \tag{A1.3a}$$

and

$$x^3 + [(1+b)\alpha + 1]x^2 + (\alpha b + \beta)x + (1+b)\alpha\beta = 0 \tag{A1.3b}$$

For all parameter values considered in this paper there exist two complex and one real eigenvalues both for $\mathbf{D}_0$ and $\mathbf{D}_1$; we denote them by $\sigma_i \mp j\omega_i$ and γ_i, respectively, where $i = 0$ or 1.

(c) By linear coordinate changes the vector field matrices for the domains $\mathbf{D}_0$ and $\mathbf{D}_1$ are transformed to the real Jordan form

$$\mathbf{A}_i = \begin{bmatrix} \sigma_i & -\omega_i & 0 \\ \omega_i & \sigma_i & 0 \\ 0 & 0 & \gamma_i \end{bmatrix}, \quad i = 0, 1. \tag{A1.4}$$

These coordinate transformations are given by the relations $\mathbf{A}_i = \mathbf{T}_i\mathbf{C}_i\mathbf{T}_i^{-1}$, where the $\mathbf{T}_i$ matrices are constructed according to the rules:

(i) the first column is the real part of the complex eigenvector relating to $\sigma \mp \mathbf{j}\omega$;
(ii) the second column is the negative imaginary part of the same complex eigenvector;
(iii) the third column is the eigenvector corresponding to γ. Explicitly:

$$\mathbf{T}_i = \begin{bmatrix} s_i\left(t_i l_i - \frac{q_i+1}{\omega_i} r_i\right) & s_i t_i q_i & s_i\left(t_i - \frac{d_i}{\alpha} r_i\right) \\ s_i\left(r_i l_i + \frac{q_i+1}{\omega_i} t_i\right) & s_i r_i q_i & s_i\left(r_i + \frac{d_i}{\alpha} t_i\right) \\ \frac{-\sigma_i}{\omega_i} s_i & s_i & \frac{-\beta}{\alpha\gamma_i} d_i s_i \end{bmatrix}, \quad i = 0, 1 \tag{A1.5}$$

where

$$l_i = \frac{-q}{\omega_i}[(c_i + 1)\alpha + \sigma_i],$$

$$d_i = [(c_i + 1)\alpha + \gamma_i], \quad c_i \begin{cases} \mathbf{a}, & i = 0 \\ \mathbf{b}, & i = 1 \end{cases}$$

$$q_i = \frac{\sigma_i^2 + \gamma_i^2 - \beta}{\beta},$$

$$t_i = \frac{l_i}{\sqrt{l_i^2 + q_i^2}},$$

$$r_i = \frac{q_i}{\sqrt{l_i^2 + q_i^2}},$$

In the $\mathbf{D}_1$ domain the old X and new X' coordinates are related via $\mathbf{X} = \mathbf{T}_1\mathbf{X}' + \mathbf{X}^C_{D1}$. For $\mathbf{D}_0$ the transformation rule is $\mathbf{X} = \mathbf{T}_0\mathbf{X}'$.

Using some arbitrariness in the definition of the eigenvectors, we have selected the matrices $\mathbf{T}_0$ and $\mathbf{T}_1$ in such a way that the U_1 plane under the normal coordinate systems takes the same form

$$U_1 : x' + y' = 1 \qquad \text{(A1.6)}$$

in both domains, $\mathbf{D}_0$ and $\mathbf{D}_1$.

(d) Now we choose the semi-plane $V : y' = 0, x' < 0$ in the $\mathbf{D}_1$ domain to be that of the Poincaré section. The coordinate system in this plane coincides with the $-x'$ and z' axes.

A.2. Poincaré Map Computation

(a) Given an initial point (ξ, η) we obtain the initial vector $X_0 : (x_0 = -\xi, y_0 = 0, z_0 = \eta)$.

(b) The solution of Eqs. (2) in the normal coordinate system is

$$X(t) = \begin{bmatrix} x \\ y \\ z \end{bmatrix}(t) = \begin{bmatrix} e^{\sigma_1 t}\cos(\omega_1 t) & -e^{\sigma_1 t}\sin(\omega_1 t) & 0 \\ e^{\sigma_1 t}\sin(\omega_1 t) & e^{\sigma_1 t}\cos(\omega_1 t) & 0 \\ 0 & 0 & e^{\gamma_1 t} \end{bmatrix} \begin{bmatrix} x_0 \\ y_0 \\ z_0 \end{bmatrix} \qquad \text{(A1.7)}$$

Depending on initial values the orbit may return to the V plane without crossing the boundary plane U_1 or may leave the $\mathbf{D}_1$ domain. Numerically the problem is to determine whether the function

$$\phi(t) = x_0 e^{\sigma_1 t}\cos(\omega_1 t) + z_0 e^{\gamma_1 t} - 1 \qquad \text{(A1.8)}$$

has a root within the interval $(0, 2\pi)$. One of the possible ways to solve this problem is to find the maximum of the function $\phi(t)$, that is to solve the equation $\phi'(t^*) = 0$. If $\phi(t^*) < 0$, then the orbit returns to the V plane without crossing the boundary plane U_1. The Poincaré map in this case is calculated as follows:

$$\xi' = x_0 e^{\sigma_1 \frac{2\pi}{\omega_1}}, \quad \eta' = z_0 e^{\gamma_1 \frac{2\pi}{\omega_1}}. \qquad \text{(A1.9)}$$

If $\phi(t^*) \geqslant 0$, then the orbit starting at X_0 will hit the U_1 plane at some point X_1. To find this point we must solve the equation $\phi(t_0) = 0$ and find t_0 in the interval $(0, t^*)$. To solve the resulting transcendental equations one may use any standard technique, such as Newton–Raphson or others. Substituting the calculated t_0 to Eq. (A1.7) we obtain an intersection point $X_1 = X(t_0)$.

(c) The coordinates of X_1 in the normal coordinate system in the $\mathbf{D}_0$ domain are calculated by applying two subsequent linear transformations:

$$X_1'' = \mathbf{T}_0^{-1}(\mathbf{T}_1 X_1 + X^C_{D1}) \qquad \text{(A1.10)}$$

(d) Starting at the point $X_1'' : (x'', y'', z'')$ the orbit may then hit the plane U_1 or U_{-1} depending on the sign of the z'' value.

(1) Let $z'' > 0$. The orbit

$$X(t) = \begin{bmatrix} x \\ y \\ z \end{bmatrix}(t) = \begin{bmatrix} e^{\sigma_0 t}\cos(\omega_0 t) & -e^{\sigma_0 t}\sin(\omega_0 t) & 0 \\ e^{\sigma_0 t}\sin(\omega_0 t) & e^{\sigma_0 t}\cos(\omega_0 t) & 0 \\ 0 & 0 & e^{\gamma_0 t} \end{bmatrix} \begin{bmatrix} x'' \\ y'' \\ z'' \end{bmatrix} \qquad \text{(A1.11)}$$

will hit the plane U_1 at some point X_2. To find this point we must solve the transcendental equation

$$f(t_1) = x'' e^{\sigma_0 t_1}\cos(\omega_0 t_1) - y'' e^{\sigma_0 t_1}\sin(\omega_0 t_1) + z'' e^{\gamma_0 t_1} - 1 = 0 \qquad \text{(A1.12)}$$

and find the first return time t_1. Then we obtain $X_2 = X(t_1)$ from the Eq. (A1.11).

To localize the first return time we check the sign changes of the function itself and its derivative at least twice at period $T = 2\pi/\omega_0$. If the sign of the function has changed, then the root is localized. If the sign of the derivative has changed from positive to negative, then the equation $f'(t^*) = 0$ may be solved to find the point of extremum, and this point is checked as to whether the sign of the function has changed.

(2) If $z'' < 0$, then applying the inversion $X'' \to -X''$ and using the symmetry property of Eqs. (2) we reduce the problem to the case

of $z'' > 0$. We have already mentioned, that the interpretation of the iteration results is more sophisticated in this case, because at the end of each iteration we must identify, what domain we have finished at.

(e) The coordinates of the point X_2 under the normal coordinate system in the $\mathbf{D}_1$ domain are calculated by applying two subsequent linear transformations:

$$X_2'' = \mathbf{T}_1^{-1}(\mathbf{T}_0 X_2 - X_{D1}^C) \qquad \text{(A1.13)}$$

(f) The trajectory starting at the point X_2'' will hit the plane V at the point X_3:

$$(X_3 = -\sqrt{x''^2 + y''^2}\, e^{\sigma_1 t_2},\ y_3 = 0,\ z_3 = z'' e^{\gamma_1 t_2}), \qquad \text{(A1.14)}$$

where $t_2 = (\pi - \operatorname{arctg}(y_2''/x_2''))/\omega_1$.

(g) Finally, the Poincaré map is calculated as follows:

$$\xi' = -x_3, \quad \eta' = z_3. \qquad \text{(A1.15)}$$

The flow defined by the vector field (2) provides a one-to-one correspondence between the initial and the first return points at the plane V, thus we obtain the 2D map:

$$\begin{aligned} \xi' &= F(\xi, \eta) \\ \eta' &= G(\xi, \eta), \end{aligned} \qquad \text{(A1.16)}$$

which is defined by the relation (A1.15) together with (A1.9).

The typical value of the γ_1 eigenvalue is ≈ -3. Hence the trajectories contract towards the plane $z' = 0$ strongly. The dynamics of the Poincaré map evolves in a narrow band near the x' axis. We may assume $z_3 = 0$ and then obtain the approximate 1D map for Chua's system, which is defined by the equation

$$\xi' = F(\xi, 0). \qquad \text{(A1.17)}$$

This enables us to use the homotopy (11).

Appendix 2
RG Analysis of Period-Doubling Critical Behavior for 1D Maps

Consider a 1D map $X_{n+1} = G(X_n)$ having at least one extremum (maximum for definiteness) at $X = \overline{x}$. At first, we translate the origin to this point and obtain the redefined map

$$x_{n+1} = g_0(x_n), \qquad \text{(A2.1)}$$

where $x = X - \overline{x}$, $f(x) = G(x + \overline{x}) - \overline{x}$. Let us apply this map twice and rescale the x variable in such a way that the new mapping is normalized to unity at the origin.: $g_{\text{new}}(x) = a g_0(g_0(x/a))$, where $a = 1/g_0(g_0(0))$. This is *Feigenbaum's RG transformation or doubling transformation* [Feigenbaum, 1978, 1979]. Repeating this procedure many times we obtain the recurrent functional equation

$$\boxed{g_{k+1}(x) = a_k g_k\left(g_k\left(\frac{x}{a_k}\right)\right),} \qquad \text{(A2.2)}$$

where

$$a_k = \frac{1}{g_k(g_k(0))}. \qquad \text{(A2.3)}$$

The original map $g_0(x)$ is an initial condition for this equation. If this is a 1D map at Feigenbaum's critical point (say, the logistic map (2) at $\lambda_c = 1.401155\ldots$) then a functional sequence (A2.2) converges to a certain limit. This limit is *Feigenbaum's universal function*

$$\begin{aligned} g(x) = g_F(x) &= \lim f_k(x) \\ &= 1 - 1.5276x^2 + 0.1048x^4 + \cdots \end{aligned} \qquad \text{(A2.4)}$$

and

$$a = a_F = \lim a_k = \frac{1}{g_F(1)} = -2.502907876\ldots \qquad \text{(A2.5)}$$

Apparently, $g(x)$ is a fixed point of the functional equation, i.e.

$$g(x) = a g\left(g\left(\frac{x}{a}\right)\right). \qquad \text{(A2.6)}$$

Let us turn to another case and consider bimodal map $g_0(x)$. Assuming that it depends on two control parameters we may find the binary tree in the parameter plane and localize a codimension-2 critical point for a certain *UD*-code. If we take the map $g_0(x)$ at this point as the initial condition for Eq. (A2.2) we observe that the behavior of the functional sequence $g_k(x)$ depends on the *UD*-code.

For codes with a tail consisting of letters U, the sequence of functions $g_k(x)$ converges to the new

fixed point of the *RG* equation that corresponds to the tricritical point [Chang *et al.*, 1981]:

$$g(x) = g_T(x) = \lim f_k(x) = 1 - 1.8341x^4 + 0.0130x^8 + \cdots \quad \text{(A2.7)}$$

and

$$a = a_T = \lim a_k = \frac{1}{g_T(1)} = -1.69030297\ldots \quad \text{(A2.8)}$$

The function $g_T(x)$ is as universal as Feigenbaum's function. The corresponding universality class is related actually to 1D maps with a quartic extremum. This behavior appears also if the quartic extremum occurs in an iteration of the original map.

Codes with tails consisting of repeated D's also give rise to tricritical behavior. In this case, however, the sequence $g_k(x)$ converges to the function $\overline{g}_T(x) = [g_T(\sqrt{x})]^2$. The $g_T(x)$ function could also be found if we take the origin at the minimum rather than at the maximum.

If the *UD*-code has a tail of period-K then the sequence $f_k(x)$ tends asymptotically to the same period for large K. Thus, the period-K cycle of the *RG* equation (A2.2) is responsible for the dynamics at this critical point. To find the universal functions $g_k(x)$ we may search for fixed points of the K-fold iteration of the *RG* equation

$$g(x) = ag^N\left(\frac{x}{a}\right), \quad N = 2, \quad \text{(A2.9)}$$

where $N = 2^K$ and a is a product of factors a_k over all K members of the cycle. Particular solutions are [Kuznetsov *et al.*, 1993b]:

for $UDUDUD\ldots$, $K = 2$,

$$g(x) = 1 - 2.6594x^2 - 0.4571x^4 + 2.9990x^6 + \cdots, \quad a = -4.8626451\ldots; \quad \text{(A2.10)}$$

for $UUDUUD\ldots$, $K = 3$,

$$g(x) = 1 - 2.3258x^2 - 0.4318x^4 + 1.7697x^6 + \cdots, \quad a = 8.0302676\ldots; \quad \text{(A2.11)}$$

and so on.

For critical points with random *UD*-codes the sequences $g_k(x)$ behave chaotically. In this case the result looks like chaotic functional sequences ("*RG*-chaos"), but we do not deal with such cases here (see Gambaudo *et al.* [1987], MacKay & van Zeijts [1988]).

The next step consists of investigation of the perturbed solutions for the *RG* equation.

Let us take a solution of the general equation (A2.9) for some $K \geqslant 1$ and add a small perturbation: $f_k(x) = g(x) + h(x)$, $|h(x)| \ll 1$. We may select such a function $h(x)$ that accepts only a constant multiplier δ after a K-fold *RG* transformation (A2.9).

In linear approximation we obtain the following eigenproblem

$$\delta h(x) = Mh(x), \quad \text{(A2.12)}$$

where M is the linear operator

$$Mh(x) = a\left\{F_0^{N-1}(x)h\left(\frac{x}{a}\right) + \sum_{i=1}^{N-2} F_i(x)h\left(g^i\left(\frac{x}{a}\right)\right) + h\left(g^{N-1}\left(\frac{x}{a}\right)\right)\right\}, \quad \text{(A2.13)}$$

$$F_i^{N-1}(x) = \left\{\frac{d[g^{N-i-1}(\xi)]}{d\xi}\right\}_{\xi=g^{i+1}(x/a)}$$

$$N = 2^K, \quad K = 1, 2, 3\ldots$$

(Dealing with fixed points we must substitute $K = 1$.)

The essential eigenvalues δ that are larger than unity in absolute value must be found for each type of criticality. Their number determines the number of control parameters necessary to restore the perturbed criticality. In other words, this is the *codimension* of the critical situation.

For *Feigenbaum's fixed point*, the unique essential eigenvalue $\delta = \delta_F = 4.669201\ldots$ exists and was found from the numerical solution of the eigenproblem [Feigenbaum, 1978, 1979].

For the *tricritical fixed point*, there are three essential eigenvalues [Chang *et al.*, 1981; Kuznetsov, 1993], namely

$$\delta_1 = 7.284686217\ldots, \quad \delta_2 = a^2, \quad \delta_3 = a^3, \quad \text{(A2.14)}$$

where $a = -1.6903\ldots$. The first two eigenvectors relate to the even subspace ($h_{1,2}(x) = h_{1,2}(-x)$); the third one has a non-vanishing odd part ($h_3(x) - h_3(-x)(g_T'(x)/x^2)$.

For all cycles of the *RG* equation with periods $K \geqslant 2$ we have only two essential eigenvalues both

of which appear to be related to the even subspace. In particular,

for $UDUDUD\ldots$, $K = 2$,

$$\delta_1 = 35.9286114\,, \quad \delta_2 = 14.5957450\,, \qquad \text{(A2.15)}$$

for $UUDUUD\ldots$, $K = 3$,

$$\delta_1 = 244.768707\,, \quad \delta_2 = 46.2910330\,. \qquad \text{(A2.16)}$$

Appendix 3
RG Analysis of Two Period-Doubling Systems with a Unidirectional Coupling

Let us consider the model mapping

$$x_{n+1} = g_0(x_n)\,, \quad y_{n+1} = f_0(x_n, y_n)\,. \qquad \text{(A3.1)}$$

We can identify two subsystems: The first one (variable x) acts onto another (variable y), but the backward influence is absent. It is supposed that both functions $g_0(x)$ and $f_0(x, y)$ may be controlled by some parameters. To be definite, we will investigate the particular system (14) which belongs to this class.

Let us apply the mapping twice and change the scales of both variables x and y to normalize the new functions to unity at the origin. This will be a generalization of Feigenbaum's *RG* transformation for systems with a unidirectional coupling. A repetition of this procedure gives the recurrent *RG* equations [Kuznetsov *et al.*, 1991, 1993a]

$$g_{k+1}(x) = a_k g_k\left(g_k\left(\frac{x}{a_k}\right)\right)\,,$$
$$f_{k+1}(x, y) = b_k f_k\left(g_k\left(\frac{x}{a_k}\right), f_k\left(\frac{x}{a_k}, \frac{y}{b_k}\right)\right)\,, \qquad \text{(A3.2)}$$

where

$$a_k = \frac{1}{g_k(g_k(0))}\,, \quad b_k = \frac{1}{f_k(g_k(0), f_k(0, 0))}\,. \qquad \text{(A3.3)}$$

For fixed points of the *RG* equation that may be responsible for the critical behavior, Eqs. (14) yield

$$g(x) = a g\left(g\left(\frac{x}{a}\right)\right)\,,$$
$$f(x, y) = b f\left(g\left(\frac{x}{a}\right), f\left(\frac{x}{a}, \frac{y}{b}\right)\right)\,, \qquad \text{(A3.4)}$$

and

$$a = \frac{1}{g(1)}\,, \quad b = \frac{1}{f(1, 1)}\,. \qquad \text{(A3.5)}$$

The first equation coincides with (A2.6), so we may choose the known Feigenbaum's solution

$$g(x) = g_F(x)\,, \quad a = a_F = -2.5029\ldots \qquad \text{(A3.6)}$$

A simple particular solution of the second equation may be found if we suppose that the function $f(x, y)$ does not depend on the first argument. Then the equation for f also reduces to Feigenbaum's form, and we obtain

$$f(x, y) \equiv g_F(y)\,, \quad b = a_F = -2.5029\ldots\,. \qquad \text{(A3.7)}$$

Evidently, we have obtained the fixed point of the *RG* equations that corresponds to a *double Feigenbaum's point DF.*

Now let us turn to *bicriticality.* Using the model map (14) at the bicritical point as an initial condition, we observe that a sequence of function pairs $\{g_k, f_k\}$ converges to a fixed point of the *RG* transformation [Kuznetsov *et al.*, 1991]:

$$\begin{aligned} g(x) &= g_F(x) = \lim g_k(x) \\ &= 1 - 1.5276x^2 + 0.1048x^4 + \cdots \\ f(x) &= f_B(x, y) = \lim f_k(x, y) \\ &= 1 - 0.5969x^2 - 0.8556y^2 \\ &\quad - 0.0322x^4 - 0.3029x^2y^2 \\ &\quad - 0.4317y^4 + \cdots\,, \end{aligned} \qquad \text{(A3.8)}$$

$$\begin{aligned} a &= \lim a_k = a_F = -2.5029\ldots\,, \\ b &= \lim b_k = b_B = -1.505318159\ldots \end{aligned} \qquad \text{(A3.9)}$$

This solution may be found directly from Eqs. (A3.4) without any reference to the particular original map. So, *bicriticality is a universal type of behavior in period-doubling systems with a unidirectional coupling.*

Next, we have to study small perturbations of the *RG* equation solution near the fixed points (A3.6, A3.7) and (A3.8, A3.9). It is important to note that we consider here *only perturbations which do not violate the unidirectional nature of coupling.*

For the double Feigenbaum's point we substitute

$$\{g_k(x), f_k(x, y)\} = \{g(x) + \delta^k u(x), g(y) + \delta^k v(x, y)\},$$
$$g(x) = g_F(x)\,, \quad a_k = b_k = a = a_F\,,$$

and obtain the following eigenproblem:

$$\delta u(x) = a\left[g'\left(g\left(\frac{x}{a}\right)\right)u\left(\frac{x}{a}\right) + u\left(g\left(\frac{x}{a}\right)\right)\right],$$

$$(v(x, y)) = a\left[g'\left(g\left(\frac{y}{b}\right)\right)v\left(\frac{x}{a}, \frac{y}{b}\right) + v\left(g\left(\frac{x}{a}\right), g\left(\frac{y}{b}\right)\right)\right]. \tag{A3.10}$$

Since both equations are decoupled, they give independent contributions to the eigenvalue spectrum.

The first equation is known from Feigenbaum's theory and gives a unique essential eigenvalue $\delta = \delta_F = 4.6692\ldots$. The eigenfunctions of the second equation may or may not depend on x. Among the second class we have again one essential solution with the eigenvalue δ_F. There exist two solutions that depend on both arguments x and y [Kuznetsov, 1985]; they have eigenvalues $a_F = -2.5029\ldots$ and 2. The first eigenfunction $v(x, y)$ contains a nonzero odd part. Hence, it does not appear in the perturbations arising in system (14) when we tune parameters away from the *DF* point. The second eigenfunction

$$v(x, y) = 1.0587x^2 - 1.0587y^2 - 0.0905x^4 + 0.0358x^2y^2 + 0.0548y^4 + \cdots \tag{A3.11}$$

is even and relevant. We conclude that in system (14) the *DF* point appears as a phenomenon of codimension-3. The eigenvalues responsible for scaling properties of the parameter space near this point are $\delta_1 = \delta_2 = \delta_F$ and $\delta_3 = 2$.

For the bicritical point we search for the perturbed solution of Eqs. (A3.2) in the form

$$\{g_k(x), f_k(x, y)\} = \{g(x) + \delta^k u(x), f(x, y) + \delta^k v(x, y)\},$$

$$g(x) = g_F(x), \quad f(x, y) = f_B(x, y),$$

$$a_k \equiv a = a_F, \quad b_k \equiv b = b_B.$$

Then we obtain the following linearized *RG* equations for the u and v components:

$$\delta u(x) = aF\left[g'\left(g\left(\frac{x}{a}\right)\right)u\left(\frac{x}{a}\right) + u\left(g\left(\frac{x}{a}\right)\right)\right],$$

$$\delta v(x, y) = b\Big[f'_x\left(g\left(\frac{x}{a}\right), f\left(\frac{x}{a}, \frac{y}{b}\right)\right)u\left(\frac{x}{a}\right) + f'_y\left(g\left(\frac{x}{a}\right), f\left(\frac{x}{a}, \frac{y}{b}\right)\right)v\left(\frac{x}{a}, \frac{y}{b}\right) + v\left(g\left(\frac{x}{a}\right), f\left(\frac{x}{a}, \frac{y}{b}\right)\right)\Big], \tag{A3.12}$$

where f'_x and f'_y are derivatives of the function $f(x, y)$ to the first and the second arguments, respectively. This eigenproblem was found to have two essential solutions. The first has a nonvanishing u-component; it is the Feigenbaum's eigenfunction with eigenvalue $\delta_1 = \delta_F$. It relates evidently to a perturbation of the control parameter in the first subsystem. Another relevant solution has a zero u-component and appears due to the parameter shift in the second subsystem. Numerical solution of the second Eq. (A3.12) gives the eigenvalue $\delta_2 = 2.39272443$ [Kuznetsov *et al.*, 1991]. Therefore, in the class of systems with a unidirectional coupling, the bicritical situation has a codimension-2. The scaling factors for the parameter space near the bicritical point are the calculated values $\delta_1 = \delta_F$ and $\delta_2 = 2.3927\ldots$.